Controlling chirality in the synthesis of 4 + 4 diastereomeric amine macrocycles derived from *trans*-1,2-diaminocyclopentane and 2,6-diformylpyridine.

Dominika Fedorowicz, Sylwia Banach, Patrycja Koza, Rafał Frydrych, Katarzyna Ślepokura, Janusz Gregoliński*

Content:

1. Building blocks

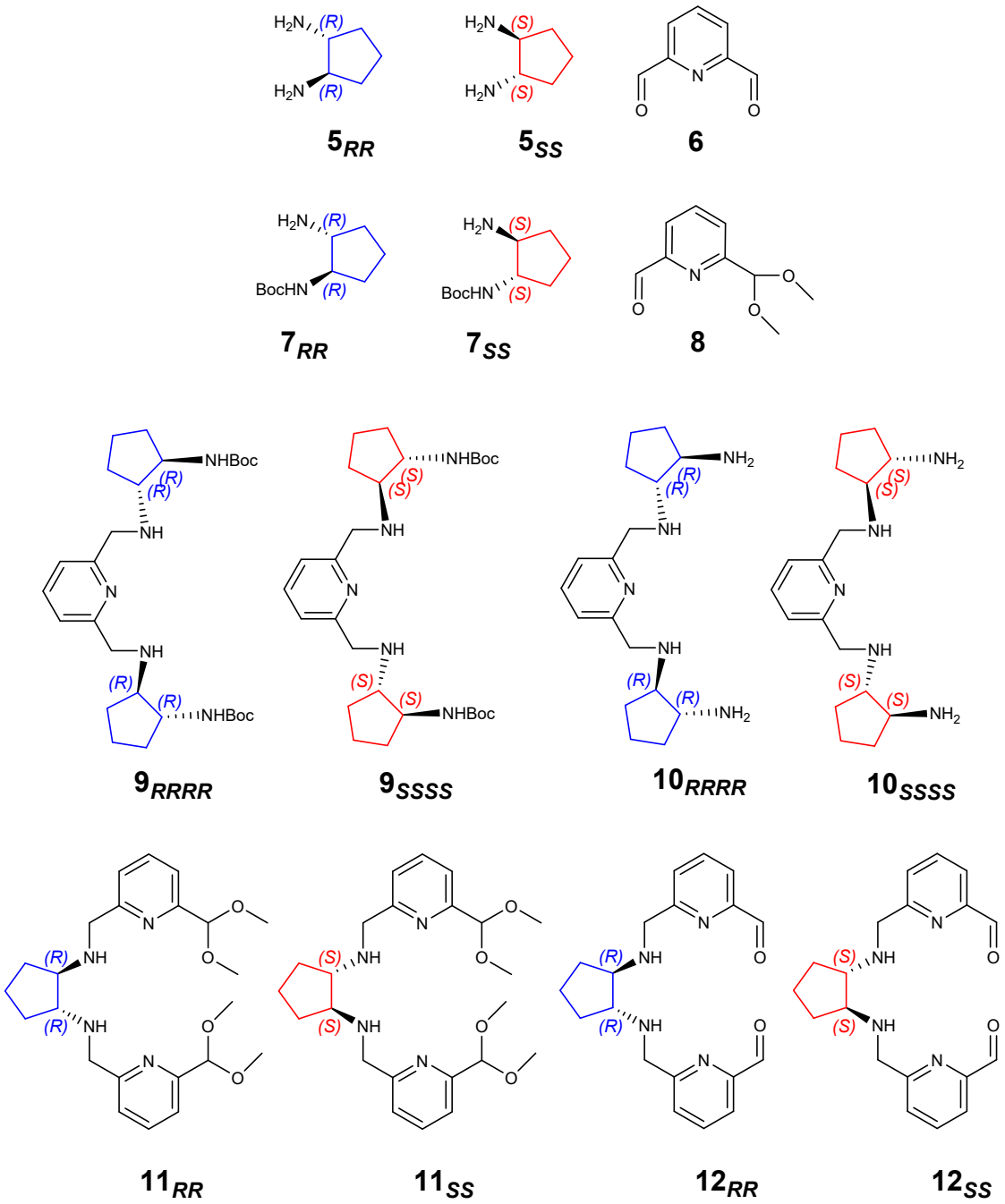

Supporting figure S1. Formulae and numeration of 1+0, 0+1, 2+1 and 1+2 building blocks.[12h]

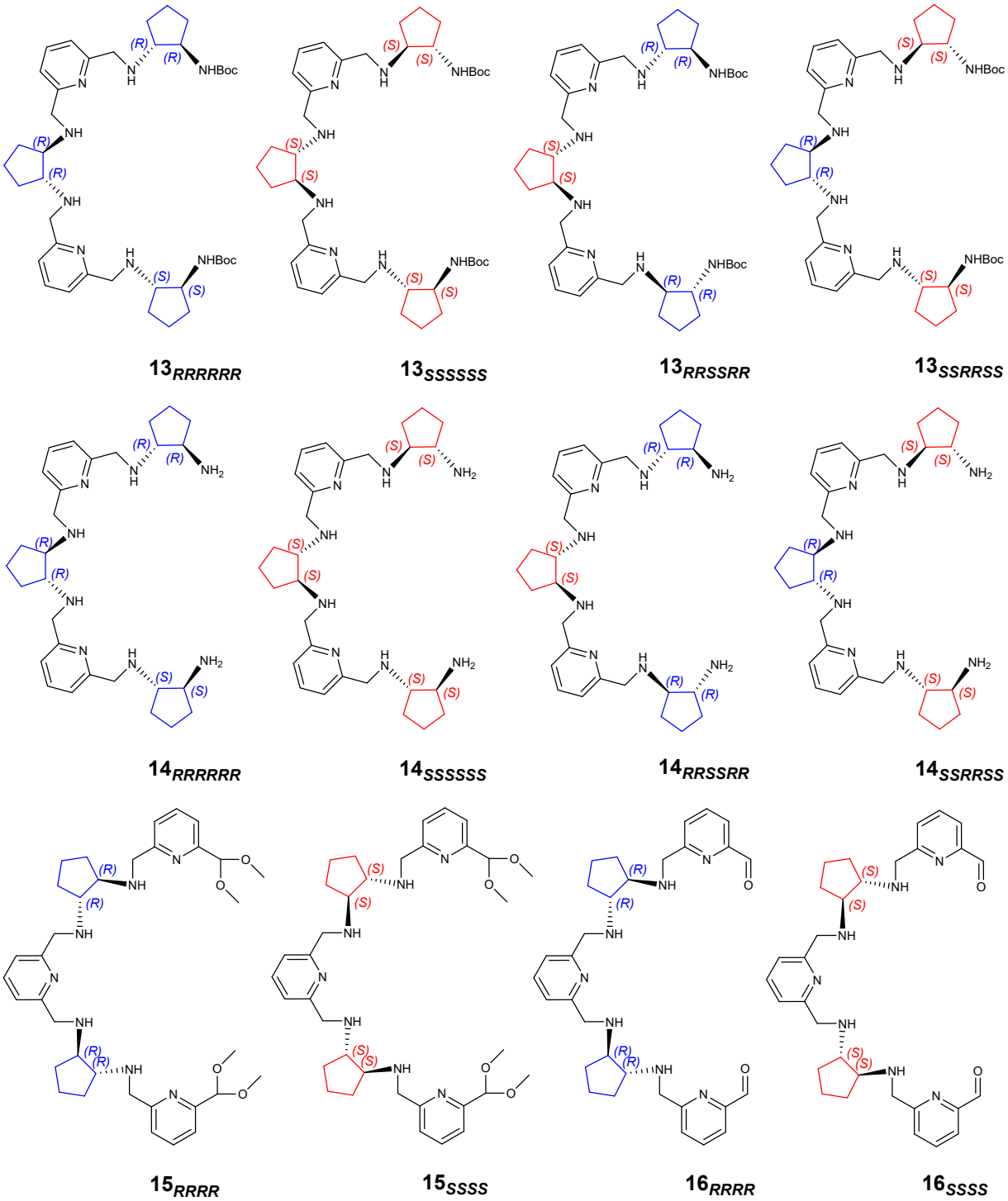

Supporting figure S2. Formulae and numeration of 3+2 and 2+3 building blocks.

2. Isomers of diimino hexaamine intermediates

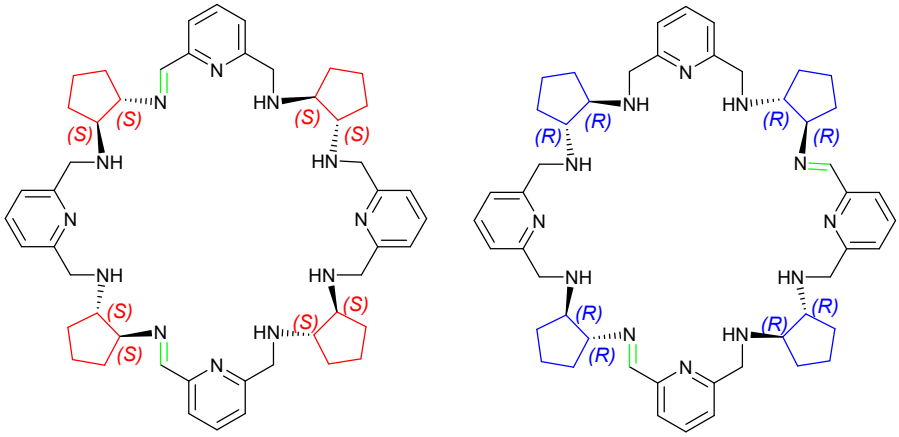

Supporting figure S3. Isomers of diimino hexaamine intermediates **1a'**$_{SSSSSSSS}$ and **1a"**$_{RRRRRRRR}$ obtained according to **reaction 1** and **2**, respectively.

3. Formation of 2+1, 1+2, 2+3 and 3+3 building blocks

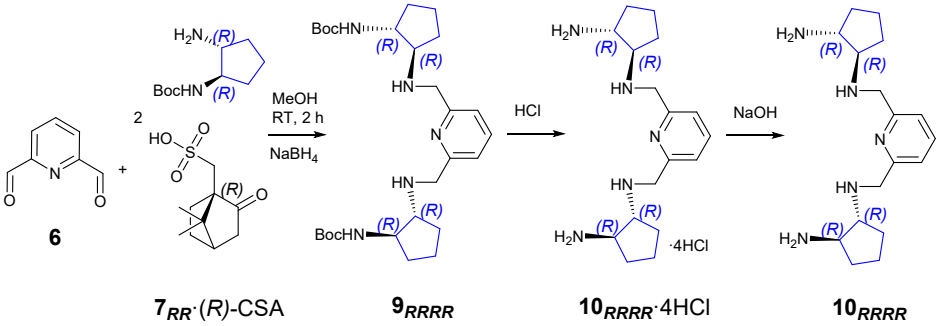

Supporting scheme S1. Synthesis of 2+1 diamine building block **10**$_{RRRR}$.

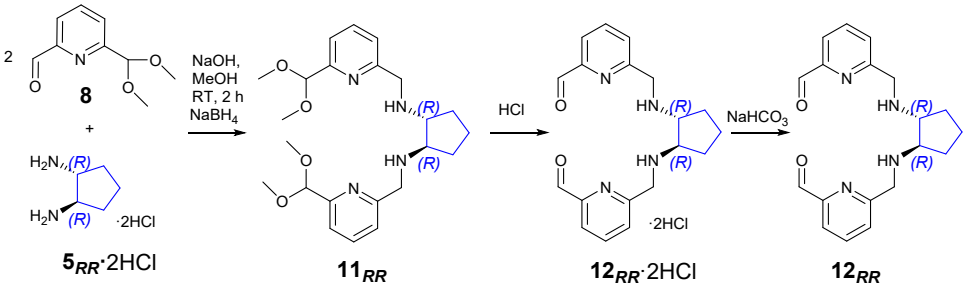

Supporting scheme S2. Synthesis of 1+2 dialdehyde building block **12**$_{RR}$.

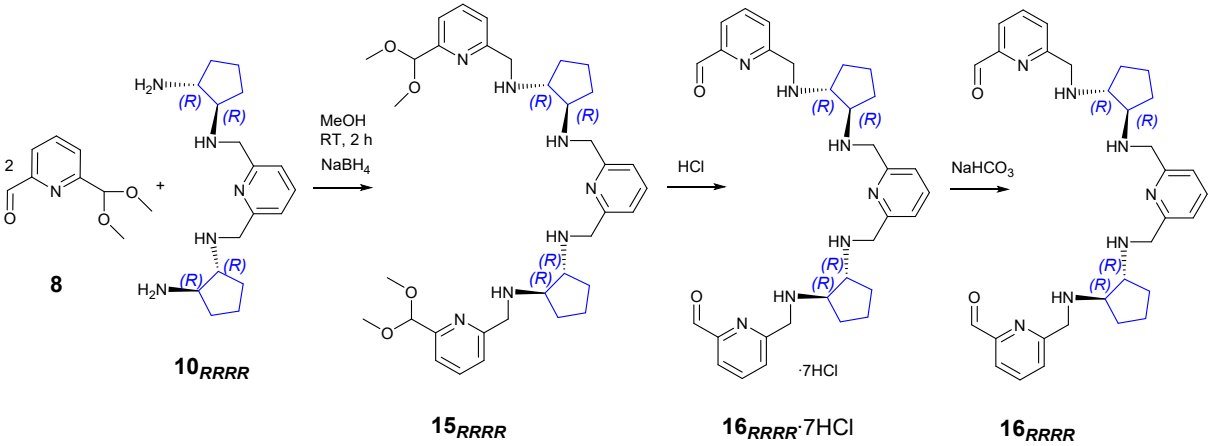

Supporting scheme S3. Synthesis of 2+3 dialdehyde building block **16**$_{RR}$.

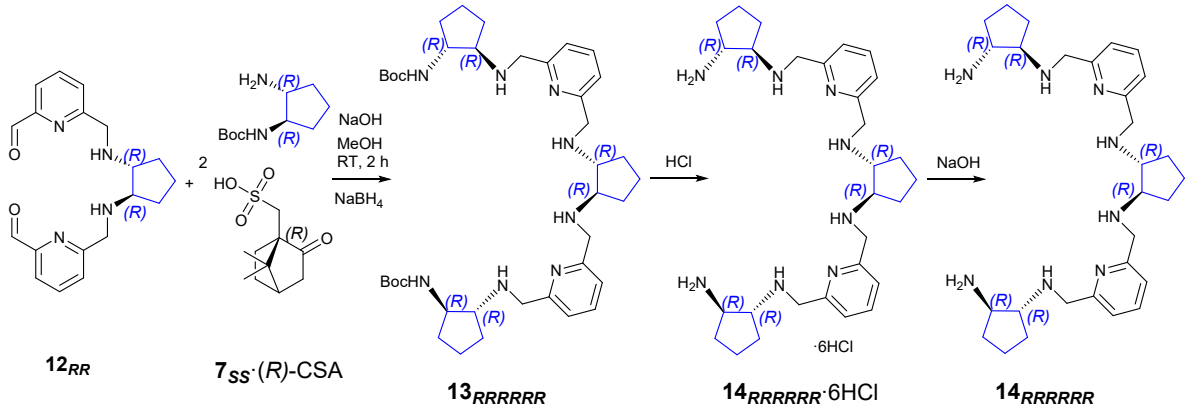

Supporting scheme S4. Synthesis of 3+2 diamine building block **14**$_{RRRRRR}$.

4. Synthesis of heterochiral 4+4 amine macrocycle $4_{SSSSSSRR}$

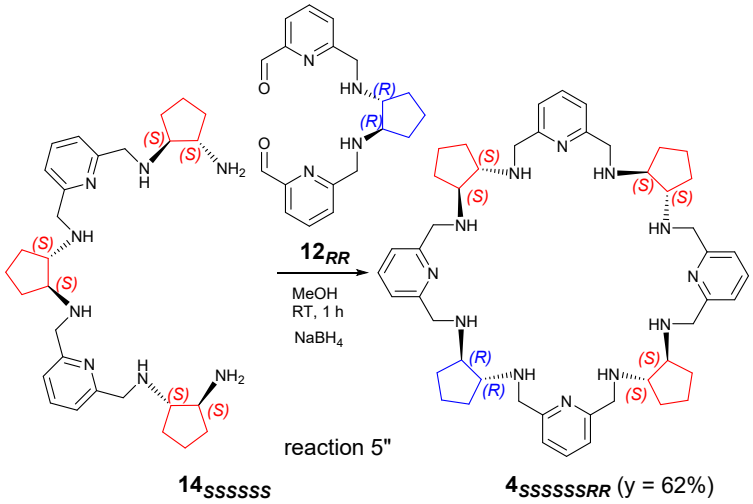

Supporting scheme S5. Synthesis of heterochiral 4+4 amine macrocycle $\mathbf{4}_{SSSSSSRR}$ from 3+2 diamine $\mathbf{14}_{SSSSSS}$ and 1+2 dialdehyde $\mathbf{12}_{RR}$ building blocks.

5. ^{1}H NMR spectra of crude macrocyclic amines 1 – 4.

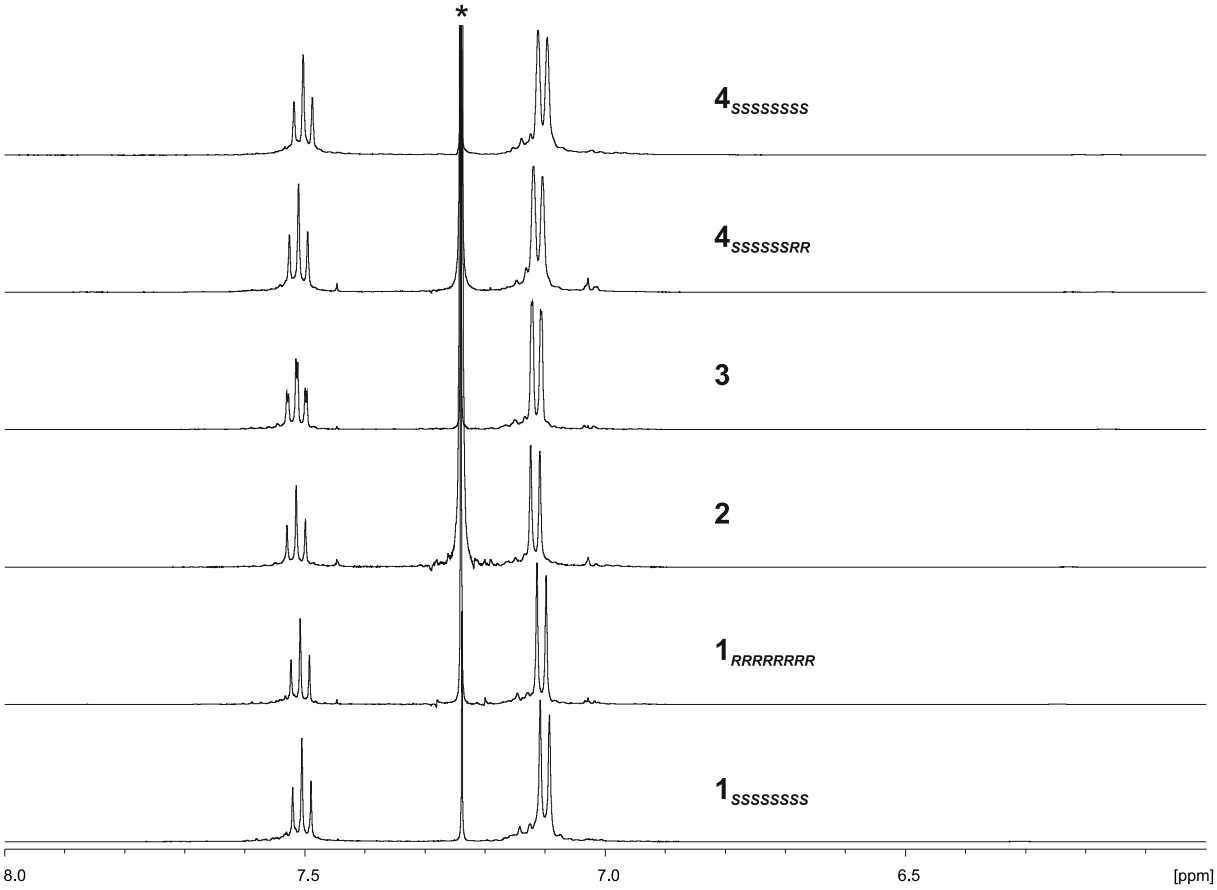

Supporting figure S4. Aromatic fragments of ^{1}H NMR spectra of crude macrocyclic amines **1**$_{SSSSSSSS}$, **1**$_{RRRRRRRR}$, **2**, **3**, **4**$_{SSSSSSRR}$ and **4**$_{RRRRRRSS}$ obtained according to **reaction 1**, **2**, **3**, **1'**, **2"** and **2'**, respectively (see the main text).

6. Crystallographic data[13]

Single crystals of [(**1**$_{SSSSSSSS}$)H_8]$(HSO_4)_{4.4}(SO_4)_{1.8}\cdot 0.8CH_3OH\cdot 7.8H_2O$ were grown by diffusion of acetonitrile to the methanol solution of 4+4 amine salt with sulfuric acid, [(**1**$_{SSSSSSSS}$)H_8]$(HSO_4)_4(SO_4)_2\cdot 16H_2O$, whereas the single crystals [(**2**)H_8]$Cl_8\cdot 11.3H_2O$ were obtained by slow evaporation from a methanol/acetonitrile solution of [(**2**)H_8]$Cl_8\cdot 8H_2O$ salt. In turn, single crystals of the chloride salt of protonated heterochiral 4+4 macrocyclic amine **3**, [(**3**)H_8]$Cl_8\cdot 3CH_3OH\cdot H_2O$ were grown by slow evaporation of methanol solution of amine salt [(**3**)H_8]$Cl_8\cdot 6H_2O$ and at last [(**4**$_{RRRRRRSS}$)H_8]$Cl_8\cdot 9H_2O$ single crystals were grown by diffusion of isopropanol to the methanol solution of 4+4 macrocyclic amine salt with hydrochloric acid [(**4**$_{RRRRRRSS}$)H_8]$Cl_8\cdot 8H_2O\cdot 2CH_3OH$.

Single-crystal X-ray diffraction data were collected at 100 K on Agilent Technologies Xcalibur, Gemini ultra (Ruby CCD detector), Rigaku XtaLAB Synergy R, DW system, (HyPix-Arc 150) or Kuma KM4-CCD (Sapphire2) *κ*-geometry diffractometers using Mo *Kα* radiation (for details see Supporting table S1). Data collections, cell refinements, data reductions and analyses were carried out with CrysAlis *PRO*[13a]. Data were corrected for Lorentz, polarization and absorption effects (analytical or empirical; multi-scan).

Crystal structures were solved using a dual-space algorithm with SHELXT-2014 program[13b], and refined on F^2 by a full-matrix least-squares method using the SHELXL-2014/7 program[13c]. All non-H atoms in [(**3**)H_8]$Cl_8\cdot 3CH_3OH\cdot H_2O$ and most of them in the remaining structures, i.e. fully occupied and with site occupation factors (SOFs) > 0.5 (or lower for Cl^- anions and some water oxygen atoms in [(**2**)H_8]$Cl_8\cdot 11.3H_2O$ and [(**4**$_{RRRRRRSS}$)H_8]$Cl_8\cdot 9H_2O$), were refined with anisotropic atomic displacement parameters.

In [(**1**$_{SSSSSSSS}$)H_8]$(HSO_4)_{4.4}(SO_4)_{1.8}\cdot 0.8CH_3OH\cdot 7.8H_2O$ three hydrogensulfate (containing S1, S3 and S5 atoms) and one sulfate anion (with S2) were refined as fully occupied and ordered. For the remaining anions a correlated disorder (or partial occupancy) was assumed (Supporting figure S5a). HSO_4^- with S6 atom was refined in two positions (with SOFs = 0.760(5) and 0.240(5)), while anionic position occupied by S4 was refined as 0.760(5) SO_4^{2-} and 0.240(5) HSO_4^-. Another position was refined as shared by HSO_4^- (S7; SOF = 0.240(5)) and methanol molecule (disordered over three positions with SOF = 0.253(2) each, which is 1/3 of 0.76). One of the water molecules (O3*W*) was refined with SOF = 0.760(5), seven remaining are fully occupied.

There are two crystallographically independent [(**4**$_{RRRRRRSS}$)H_8]$^{8+}$ cations in [(**4**$_{RRRRRRSS}$)H_8]$Cl_8\cdot 9H_2O$ (marked as *A* and *B*). Two DACP rings in cation *B*, as well as in [(**2**)H_8]$Cl_8\cdot 11.3H_2O$, were found to be disordered and were refined in two positions each, with SOFs given in CIF files. Some positions of the chloride anions in these crystals were refined as disordered or not fully occupied. Some other positions were refined as sharing their site with one or more positions of water molecules. All but one water molecules in [(**2**)H_8]$Cl_8\cdot 11.3H_2O$ are disordered or their positions are partially occupied. The same applies to many water molecules in [(**4**$_{RRRRRRSS}$)H_8]$Cl_8\cdot 9H_2O$. For details see the CIF files.

In the presented crystal structures, some geometrical restraints (DFIX, SAME instructions in the SHELXL-2014), restraints on anisotropic displacement parameters (SIMU), anti-bumping restraints (BUMP), constraints on the coordinates and U_{ij} (EXYZ and EADP), and restraints on the sum of SOFs (SUMP) were applied in the refinement procedures to get acceptable and appropriate models of the disorder.

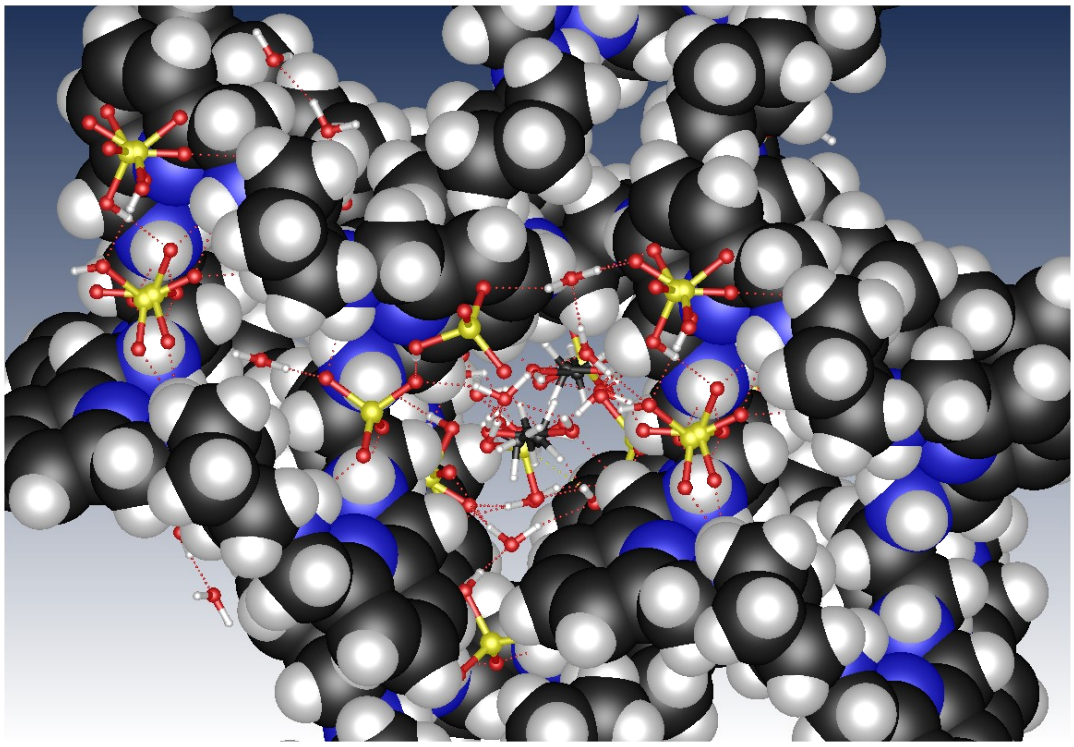

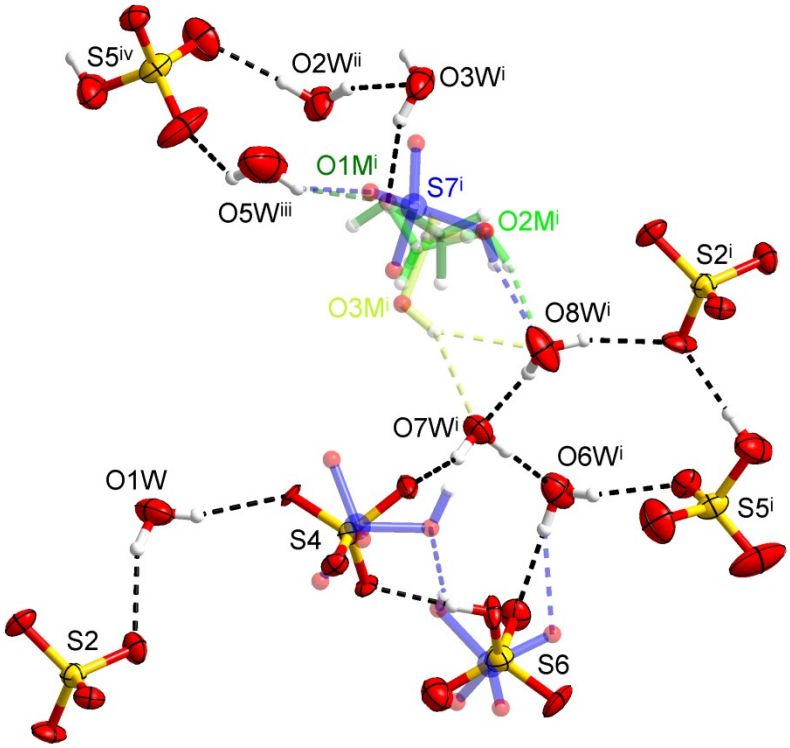

Supporting figure S5a. $[(\mathbf{1}_{sssssssss})H_8](HSO_4)_{4.4}(SO_4)_{1.8}\cdot 0.8CH_3OH\cdot 7.8H_2O$. Top: hydrogen-bonded HSO_4^- and SO_4^{2-} anions, and solvent molecules located in the voids formed by $[(\mathbf{1}_{sssssssss})H_8]^{8+}$ cations (shown as space-filling). Bottom: correlated disorder in the anionic/solvent region. Selected HSO_4^- and SO_4^{2-} anions, and solvent molecules linked by hydrogen bonds (dashed lines). Different positions are shown in different colors (blue – HSO_4^-, SOF = 0.240(5), different shades of green – MeOH, SOF = 0.253(2)). Displacement ellipsoids for anisotropically refined positions are shown at the 50% probability level. Symmetry codes: (i) x+1, y, z; (ii) –x+2, y+1/2, –z+3/2; (iii) –x+2, y–1/2, –z+3/2; (iv) –x+3/2, –y+1, z+1/2.

H atoms were included using geometrical considerations or were found in difference Fourier maps. In the final refinement cycles, C- and N-bound H atoms in all structures, as well as those from HSO_4^- anions and MeOH OH groups were repositioned in their calculated positions and refined using a riding model (or as riding rotating groups), with O–H = 0.84 Å, N–H = 0.91 Å and C–H = 0.95–1.00 Å, and with $U_{iso}(H) = 1.5U_{eq}(O)$, $1.2U_{eq}(N, C)$ for NH_2, CH and CH_2 or $1.5U_{eq}(C)$ for CH_3.

Water H atoms in [(**1**$_{SSSSSSSS}$)H_8]$(HSO_4)_{4.4}(SO_4)_{1.8}\cdot 0.8CH_3OH\cdot 7.8H_2O$ and [(**3**)H_8]$Cl_8\cdot 3CH_3OH\cdot H_2O$, and only some of them in [(**2**)H_8]$Cl_8\cdot 11.3H_2O$ and [(**4**$_{RRRRRRSS}$)H_8]$Cl_8\cdot 9H_2O$ were refined with the O–H bond lengths restrained to 0.840(2) Å, H···H distances restrained to 1.360(2) Å and then a rigid group or riding model constraints were applied (AFIX 6 or AFIX 3 instructions in SHELXL). Positions of the remaining water H atoms in [(**2**)H_8]$Cl_8\cdot 11.3H_2O$ and [(**4**$_{RRRRRRSS}$)H_8]$Cl_8\cdot 9H_2O$ were not found in difference Fourier maps.

The finally accepted formulas for the crystals are as given above and in Supporting table S1, but the amount of solvent molecules (and hydrogensulfate/sulfate anions) in [(**1**$_{SSSSSSSS}$)H_8]$(HSO_4)_{4.4}(SO_4)_{1.8}\cdot 0.8CH_3OH\cdot 7.8H_2O$, [(**2**)$H_8$]$Cl_8\cdot 11.3H_2O$ and [(**4**$_{RRRRRRSS}$)H_8]$Cl_8\cdot 9H_2O$ should be treated as a rough approximation.

Figures presenting X-ray structures were made using the Mercury[13d], *DIAMOND*[13e] and Olex[13f] programs.

The details of crystal structures refinements are given in Supporting table S1 and in the crystallographic information files (CIFs) deposited at the Cambridge Crystallographic Data Centre (CCDC Nos. 2098689-2098692) and provided as Supporting Information.

References:

See the main text.

Supporting table S1. Experimental details for the crystals.

	$[(\mathbf{1}_{SSSSSSSS})H_8](HSO_4)_{4.4}(SO_4)_{1.8}\cdot 0.8CH_3OH\cdot 7.8H_2O$	$[(\mathbf{2})H_8]Cl_8\cdot 11.3H_2O$	$[(\mathbf{3})H_8]Cl_8\cdot 3CH_3OH\cdot H_2O$	$[(\mathbf{4}_{RRRRRRSS})H_8]Cl_8\cdot 9H_2O$
CCDC No.	2098689	2098690	2098691	2098692
Chemical formula	$C_{48.8}H_{99.2}N_{12}O_{33.4}S_{6.2}$	$C_{48}H_{98.6}Cl_8N_{12}O_{11.3}$	$C_{51}H_{90}Cl_8N_{12}O_4$	$C_{48}H_{94}Cl_8N_{12}O_9$
M_r	1587.37	1308.38	1218.94	1266.95
Crystal system, space group	Orthorhombic, $P2_12_12_1$	Triclinic, $P\bar{1}$	Triclinic, $P\bar{1}$	Triclinic, $P1$
Temperature (K)	100	100	100	100
a, b, c (Å)	14.793(3), 17.860(3), 26.560(5)	13.082(2), 13.444(2), 20.564(3)	12.815(3), 14.444(3), 16.933(5)	12.441(2), 12.772(2), 20.693(4)
α, β, γ (°)	90, 90, 90	105.35(2), 108.36(2), 93.77(2)	92.83(2), 101.95(2), 90.36(2)	75.36(2), 79.83(2), 89.70(2)
V (Å^3)	7017(2)	3265.9(10)	3062.2(13)	3128.6(10)
Z	4	2	2	2
Radiation type	Mo $K\alpha$	Mo $K\alpha$	Mo $K\alpha$	Mo $K\alpha$
μ (mm^{-1})	0.30	0.41	0.42	0.42
Crystal size (mm)	0.30 × 0.03 × 0.03	0.18 × 0.10 × 0.04	0.38 × 0.31 × 0.09	0.20 × 0.03 × 0.03
Diffractometer	Agilent Technologies Xcalibur, Gemini ultra	Rigaku XtaLAB Synergy R, DW system	Kuma KM4-CCD	Rigaku XtaLAB Synergy R, DW system
Absorption correction	Analytical	Multi-scan	Multi-scan	Multi-scan
T_{min}, T_{max}	0.968, 0.992	0.879, 1.000	0.887, 1.000	0.851, 1.000
No. of measured, independent and observed [$I > 2\sigma(I)$] reflections	19757, 12675, 7169	77389, 12837, 10945	25924, 11983, 8839	126831, 24381, 21727
R_{int}	0.060	0.030	0.058	0.034
$(\sin\theta/\lambda)_{max}$ (Å^{-1})	0.606	0.617	0.617	0.617
$R[F^2 > 2\sigma(F^2)]$, $wR(F^2)$, S	0.079, 0.185, 1.00	0.061, 0.170, 1.02	0.056, 0.154, 1.00	0.058, 0.160, 1.04
No. of reflections	12675	12837	11983	24381
No. of parameters	967	854	685	1472
No. of restraints	109	817	3	151
H-atom treatment	H-atom parameters constrained	H-atom parameters constrained	H-atom parameters constrained	H-atom parameters constrained
$\Delta\rho_{max}$, $\Delta\rho_{min}$ (e Å^{-3})	0.90, −0.45	0.80, −0.50	0.40, −0.55	0.70, −0.73
Absolute structure parameter	−0.07(6)	–	–	0.025(8)

Computer programs: *CrysAlis PRO* (Rigaku OD, 2018, 2020), SHELXT-2014 (Sheldrick, 2015), *SHELXL2014*/7 (Sheldrick, 2015).

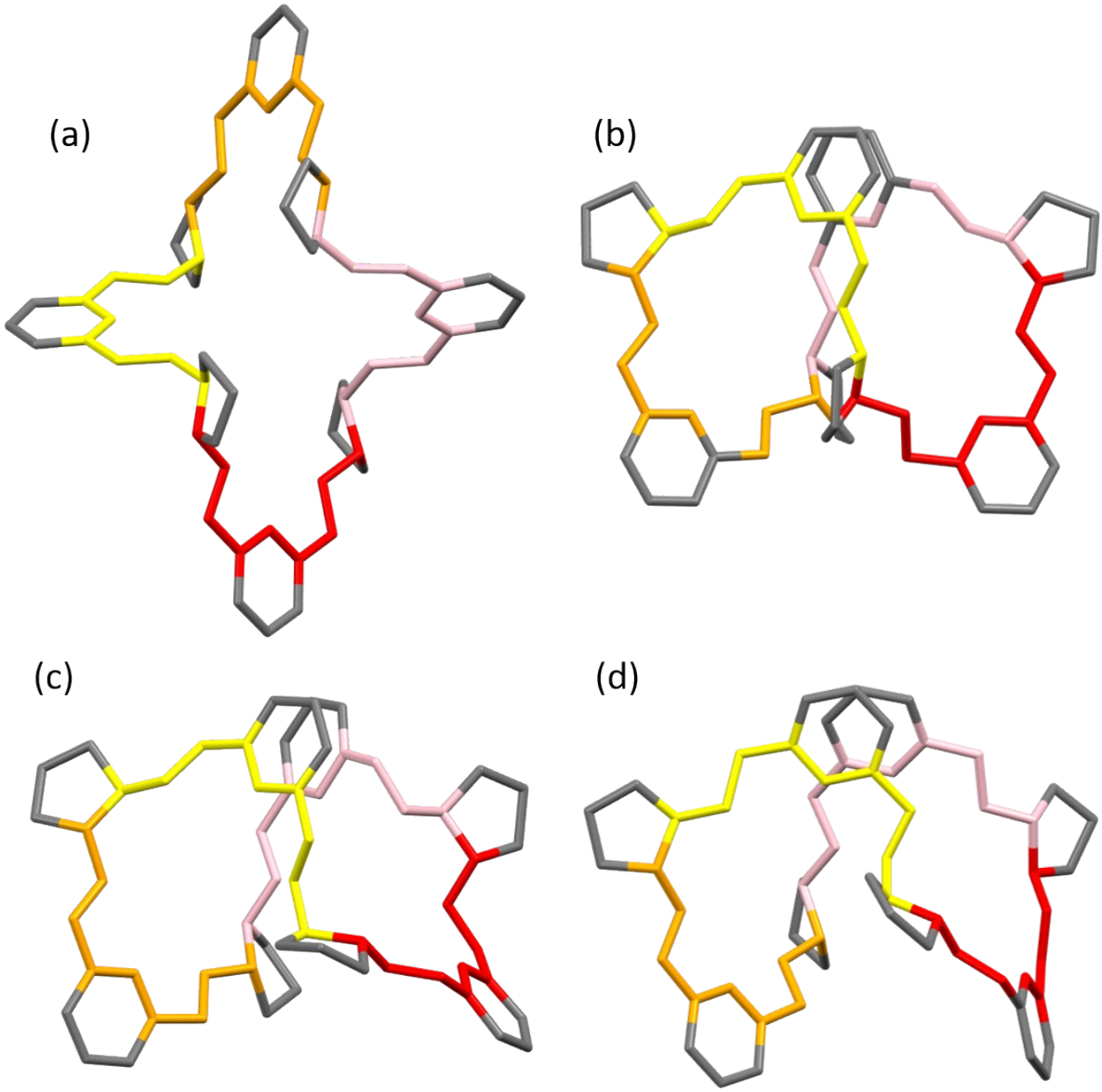

Supporting figure S5b. Four U-shaped loops (yellow-orange-pink-red) distinguished in macrocyclic amine cations: $[(\mathbf{1}_{SSSSSSSS})H_8]^{8+}$ (a), $[(\mathbf{2})H_8]^{8+}$ (b), $[(\mathbf{3})H_8]^{8+}$ (c) and $[(\mathbf{4}_{RRRRRRSS})H_8]^{8+}$(d) present in $[(\mathbf{1}_{SSSSSSSS})H_8](HSO_4)_{4.4}(SO_4)_{1.8}\cdot 0.8CH_3OH\cdot 7.8H_2O$, $[(\mathbf{2})H_8]Cl_8\cdot 11.3H_2O$, $[(\mathbf{3})H_8]Cl_8\cdot 3CH_3OH\cdot H_2O$ and $[(\mathbf{4}_{RRRRRRSS})H_8]Cl_8\cdot 9H_2O$ crystals.

7. Mass spectra

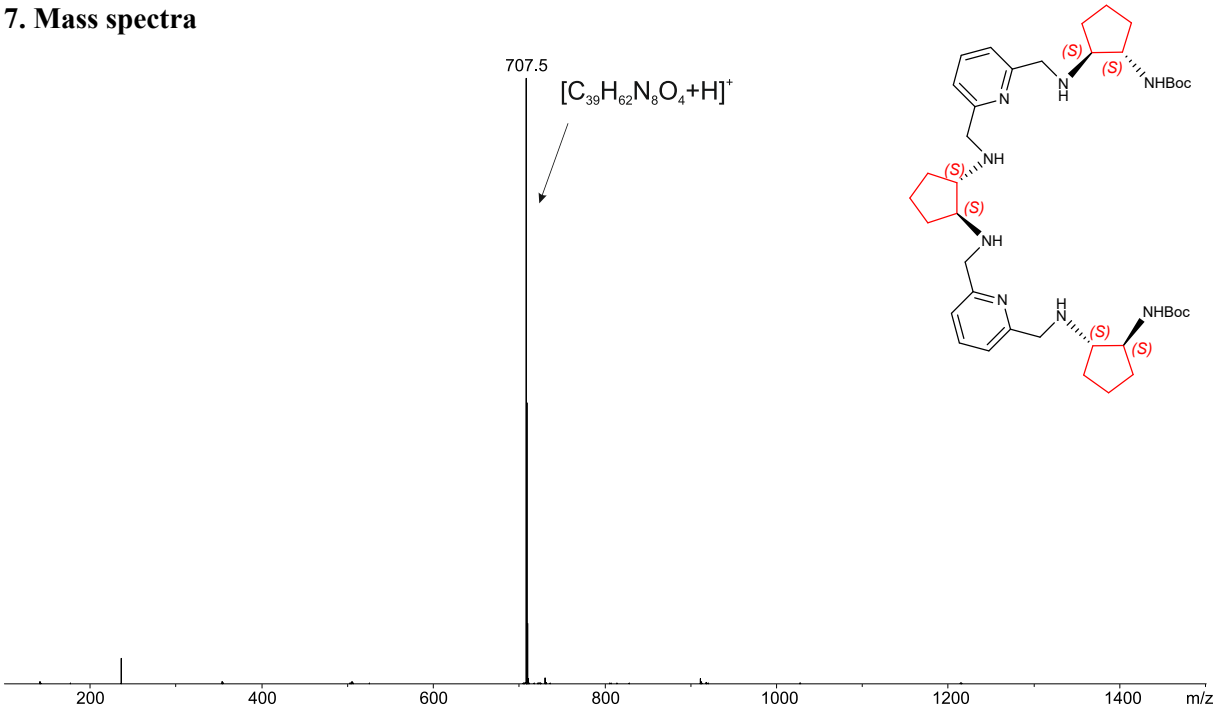

Supporting figure S6a. ESI MS spectrum of the crude di-Boc-protected primary diamine amine **13**$_{SSSSSS}$.

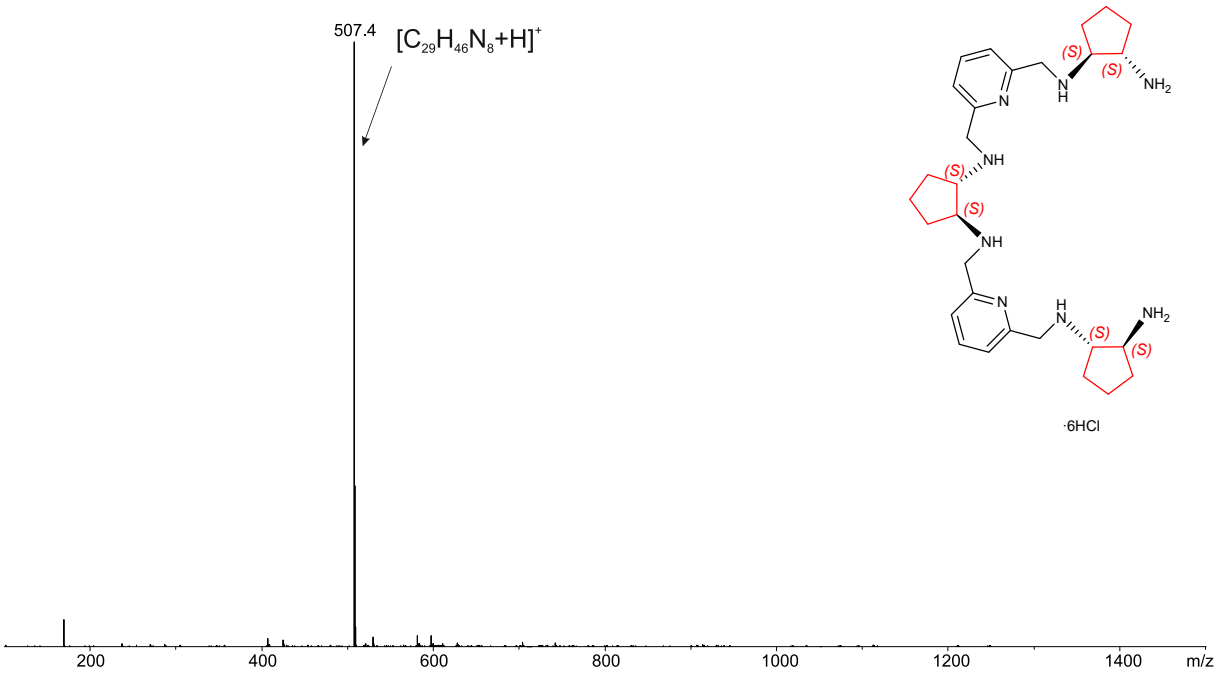

Supporting figure S6b. ESI MS spectrum of the primary diamine amine hydrochloride salt **14**$_{SSSSSS}$·6HCl·4.5H_2O.

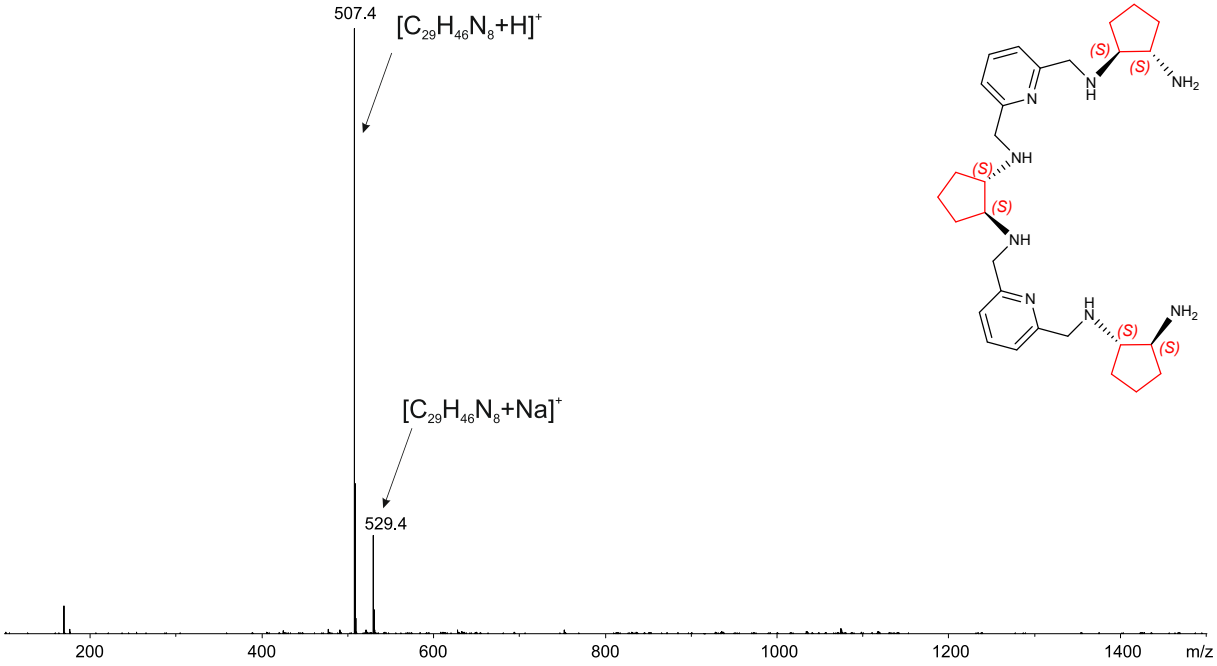

Supporting figure S6c. ESI MS spectrum of the free primary diamine amine **14**$_{sssssss}$·0.25CH_2Cl_2·0.5H_2O.

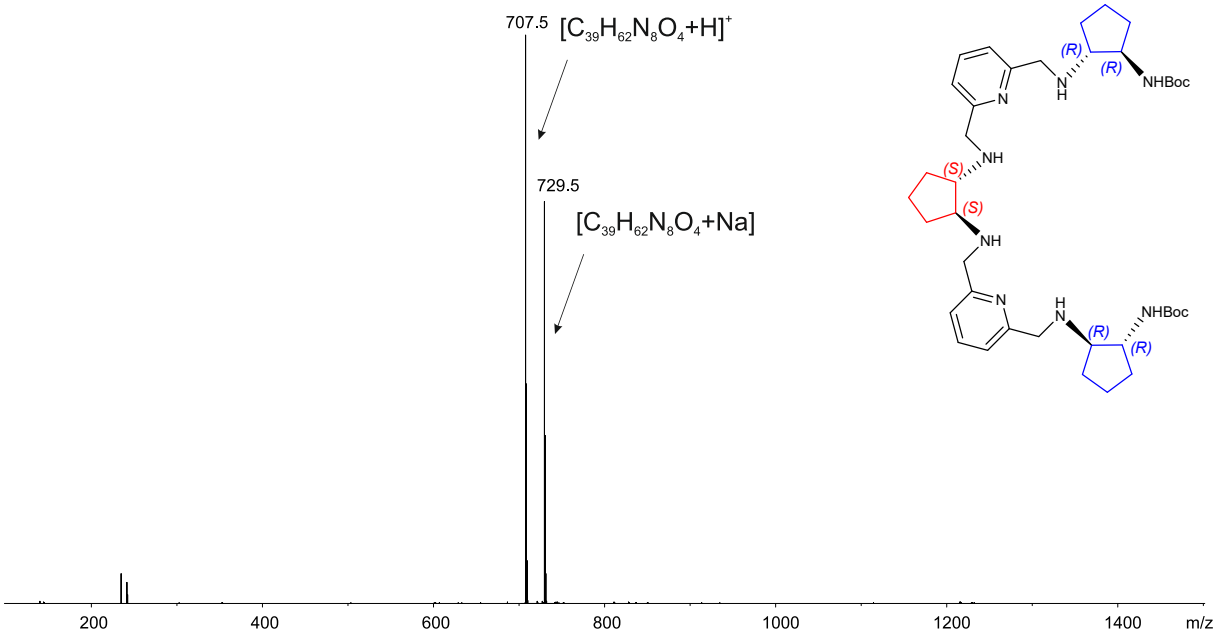

Supporting figure S7a. ESI MS spectrum of the crude di-Boc-protected primary diamine amine **13**$_{RRSSRR}$.

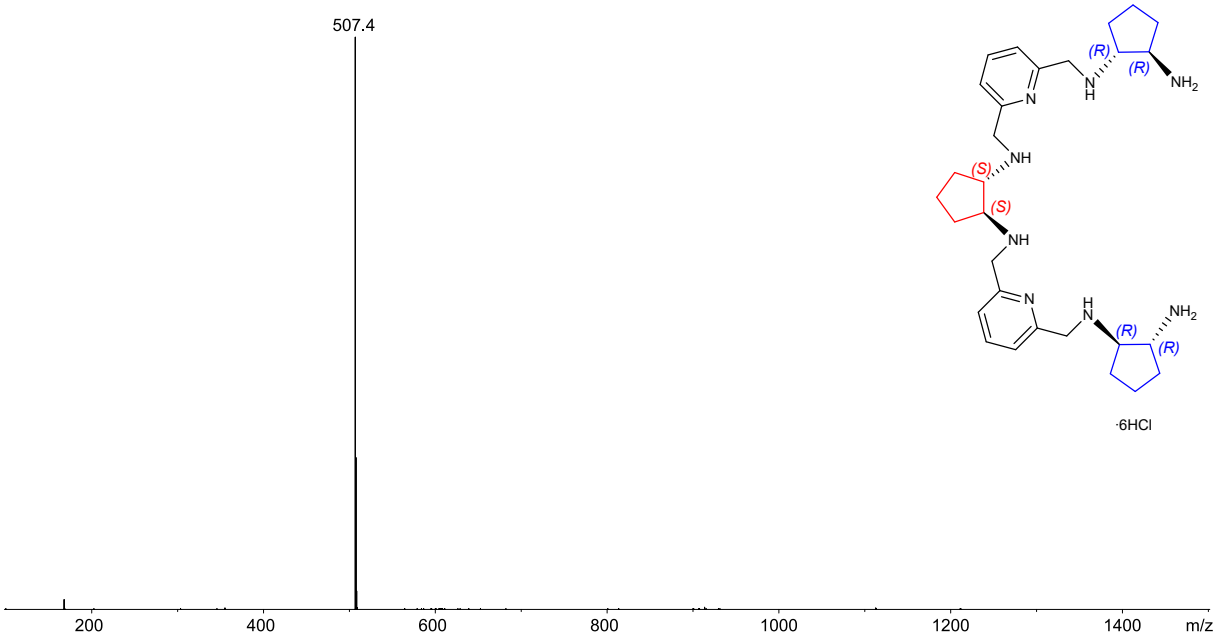

Supporting figure S7b. ESI MS spectrum of the primary diamine amine hydrochloride salt **14**$_{RRSSRR}$·6HCl·5.5H_2O.

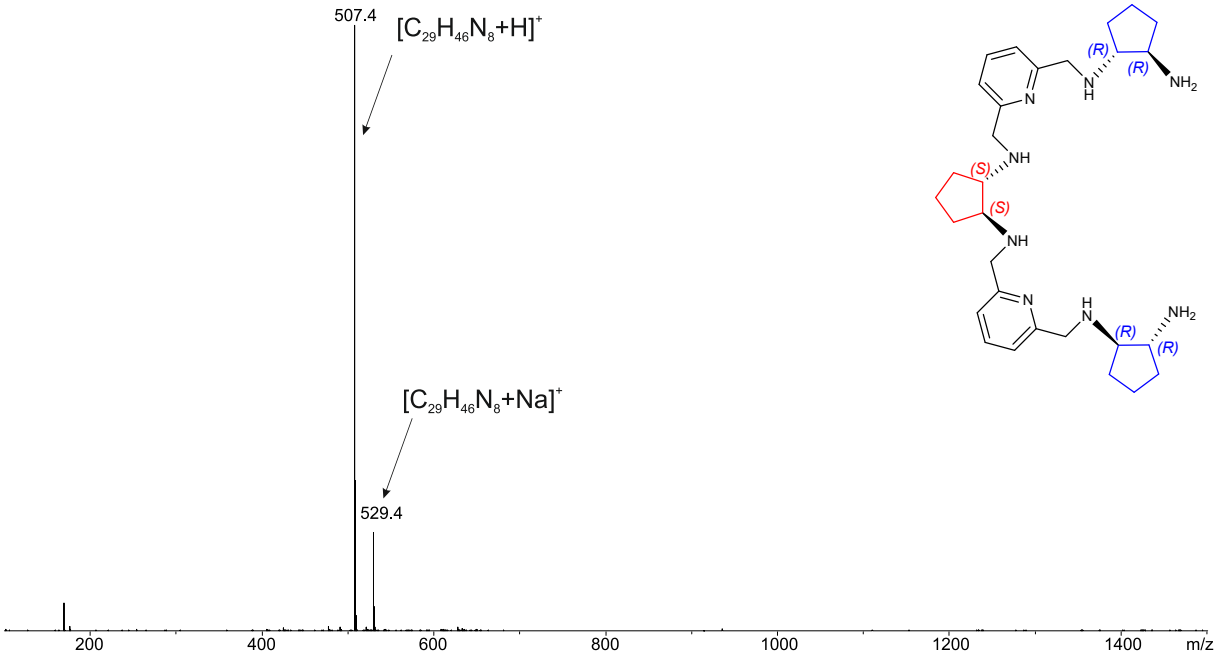

Supporting figure S7c. ESI MS spectrum of the free primary diamine amine $\mathbf{14}_{RRSSRR}\cdot 0.2CH_2Cl_2\cdot H_2O$.

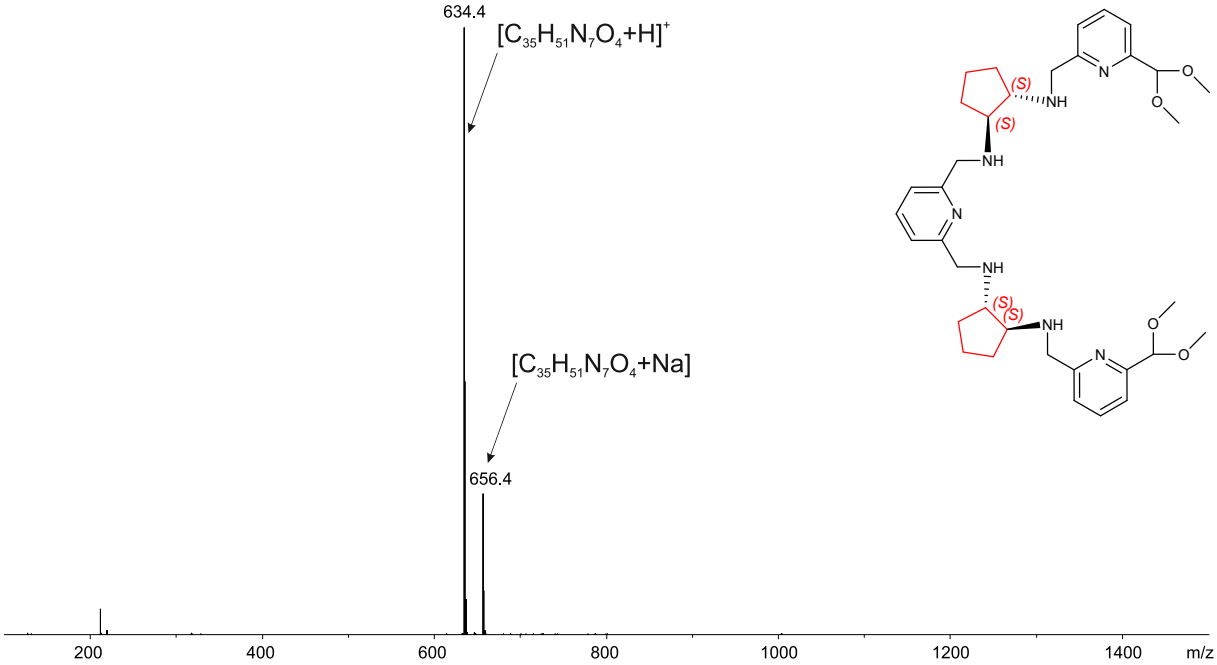

Supporting figure S8a. ESI MS spectrum of the diprotected dialdehyde **15**$_{SSSS}$·0.2$CHCl_3$·2.5H_2O.

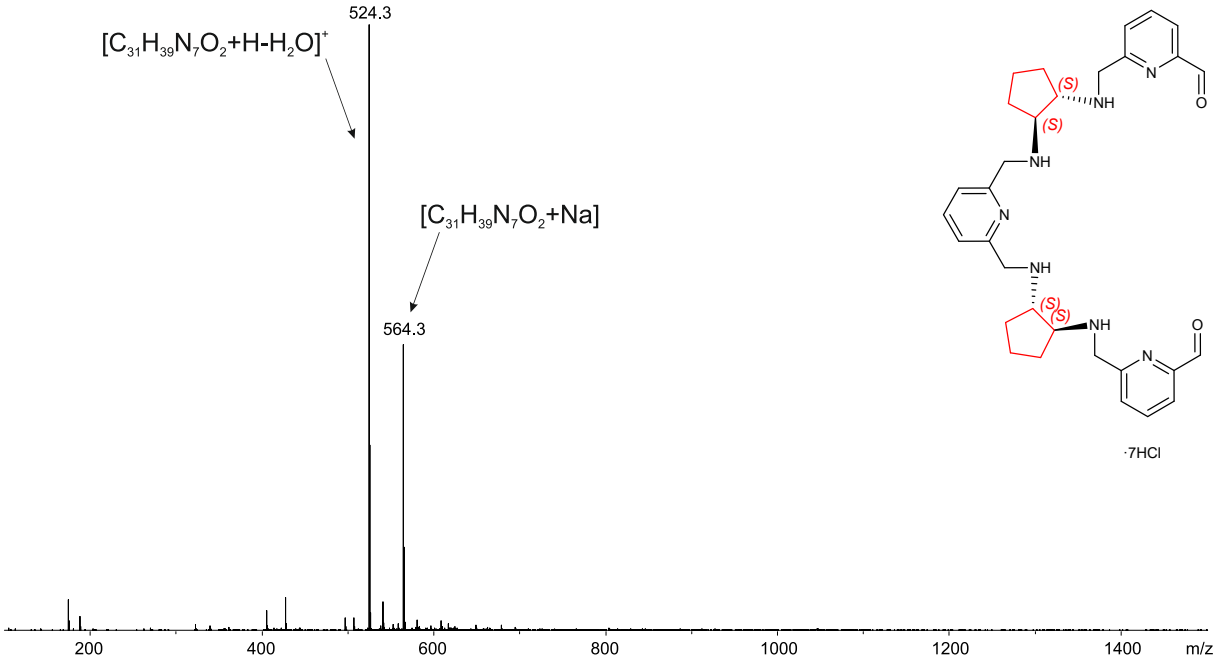

Supporting figure S8b. ESI MS spectrum of the hydrochloride salt of dialdehyde **16**$_{SSSS}$·7HCl·0.25H_2O.

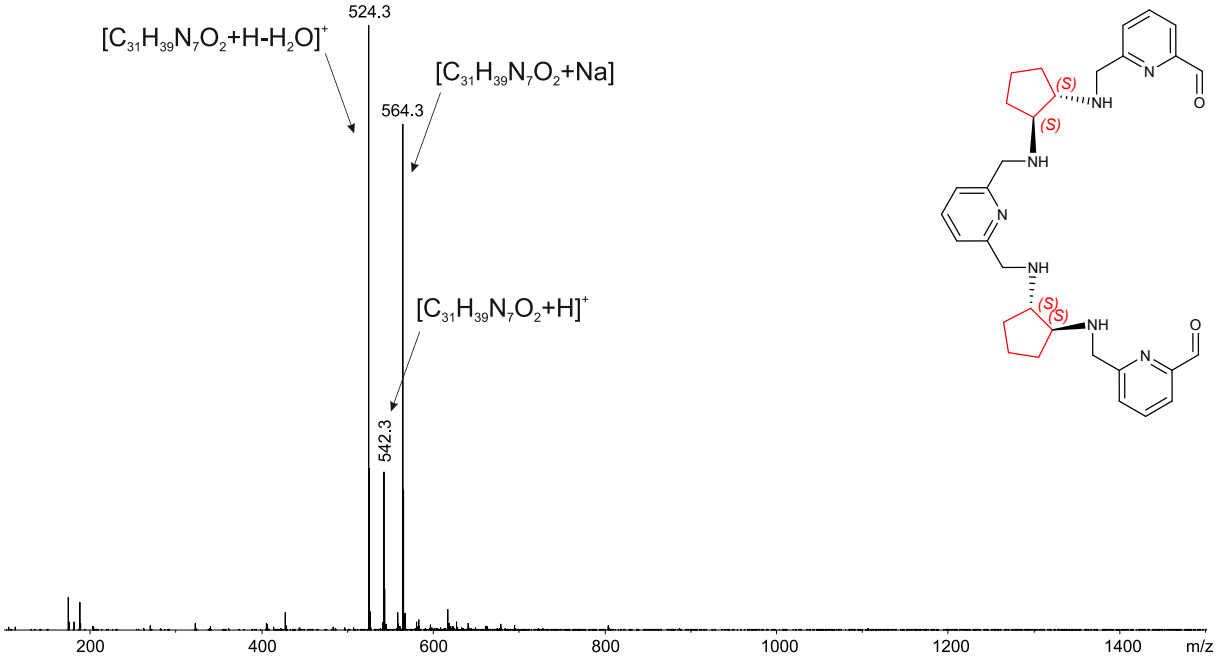

Supporting figure S8c. ESI MS spectrum of the free dialdehyde **16**$_{SSSS}$·CH_2Cl_2.

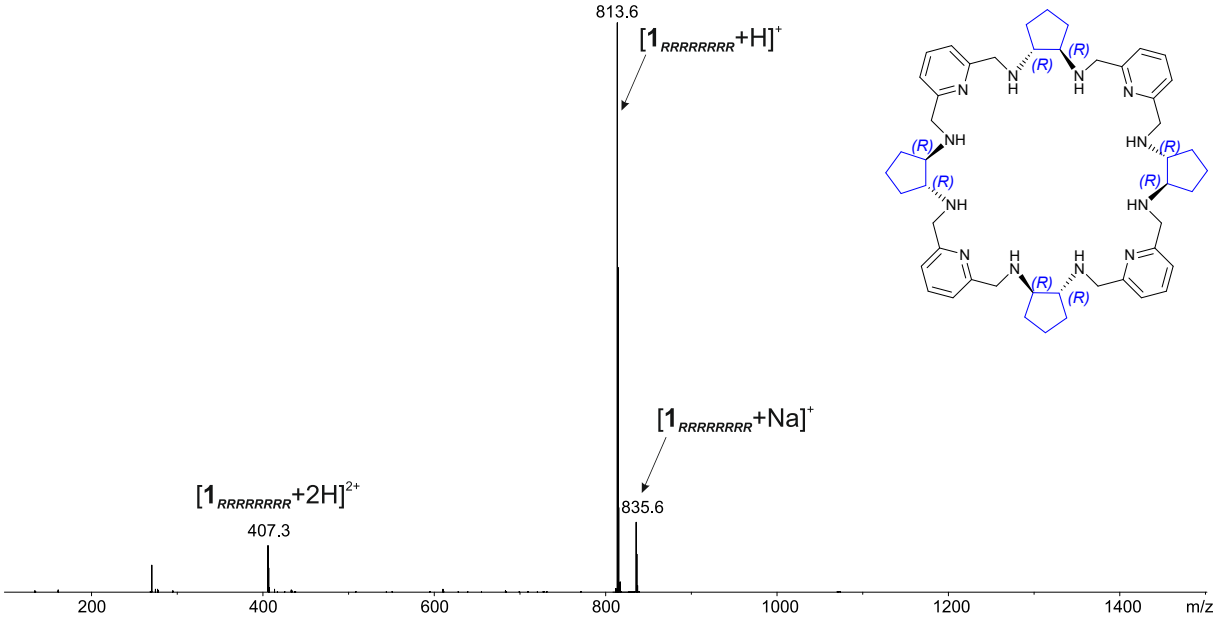

Supporting figure S9a. ESI MS spectrum of protonated salt [(**1**$_{RRRRRRRR}$)H_8]Cl_8·6H_2O.

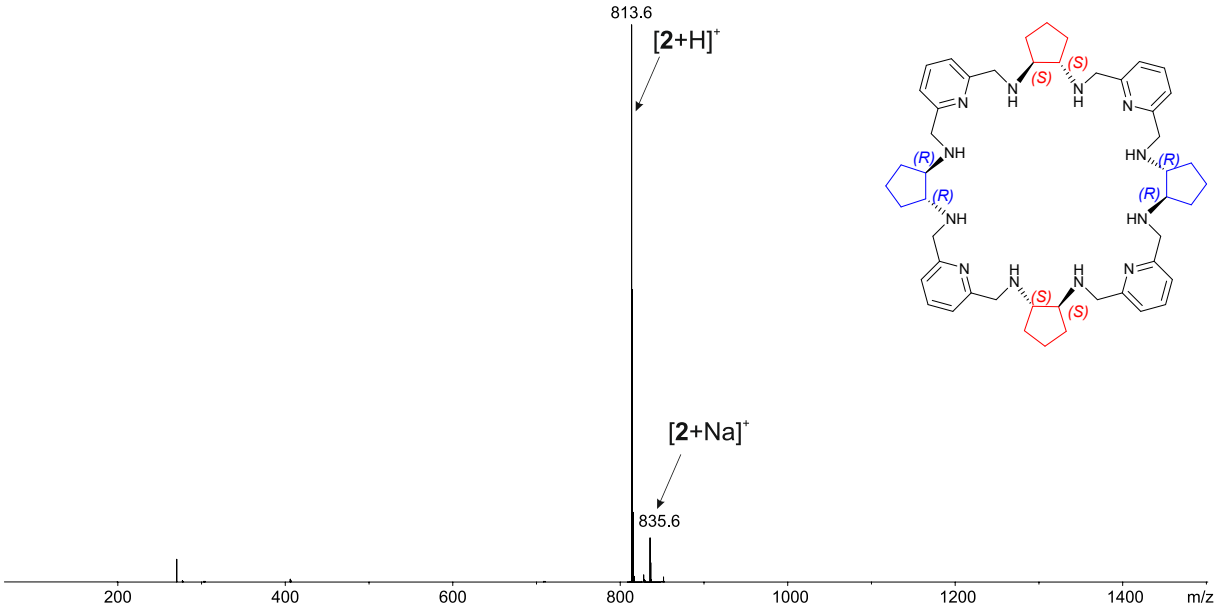

Supporting figure S9b. ESI MS spectrum of protonated salt [(**2**)H_8]Cl_8·6H_2O.

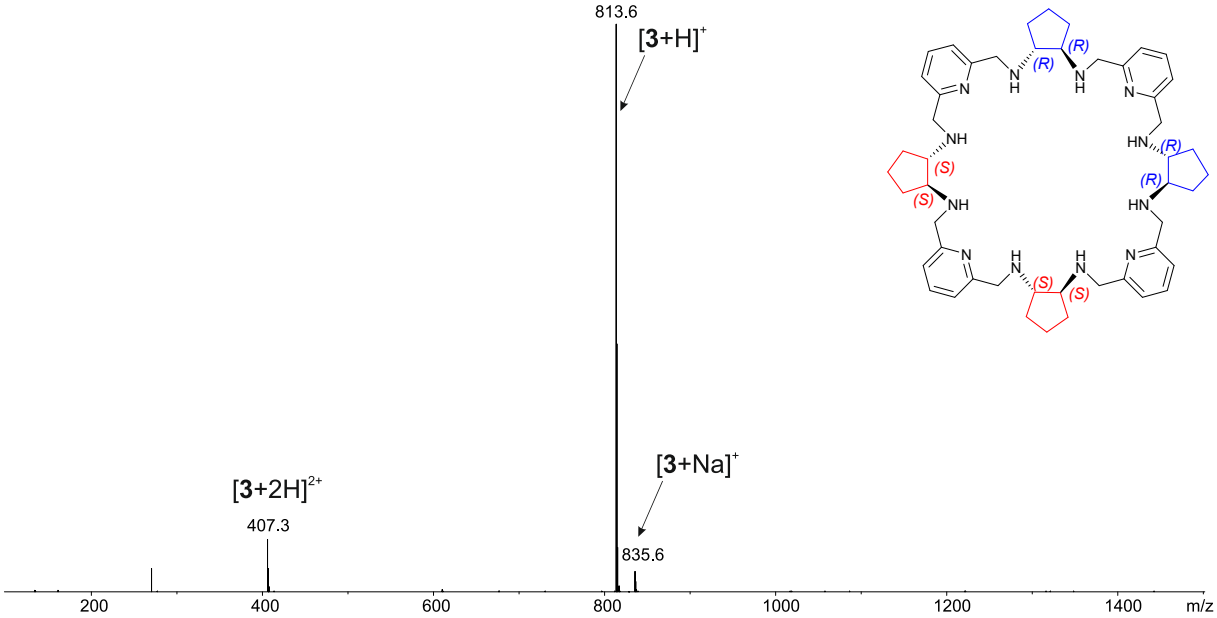

Supporting figure S9c. ESI MS spectrum of protonated salt [(**3**)H_8]$Cl_8 \cdot 6H_2O$.

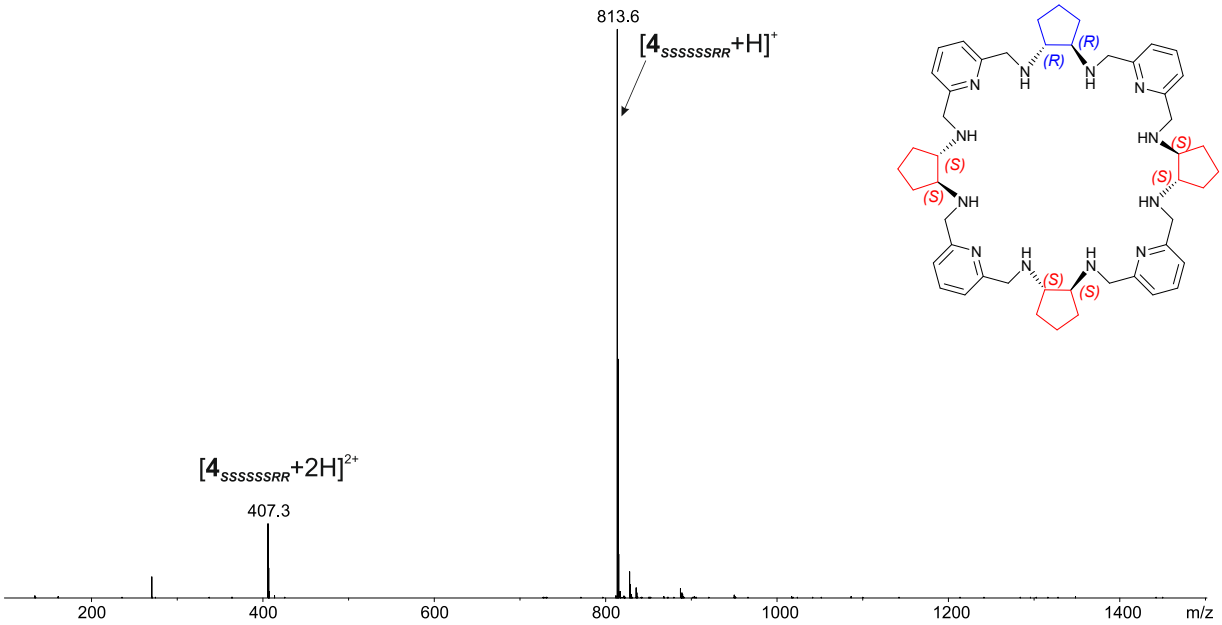

Supporting figure S9d. ESI MS spectrum of protonated salt [(**4**$_{SSSSSSRR}$)H_8]$Cl_8 \cdot 3.5H_2O$.

8. NMR spectra of pure compounds

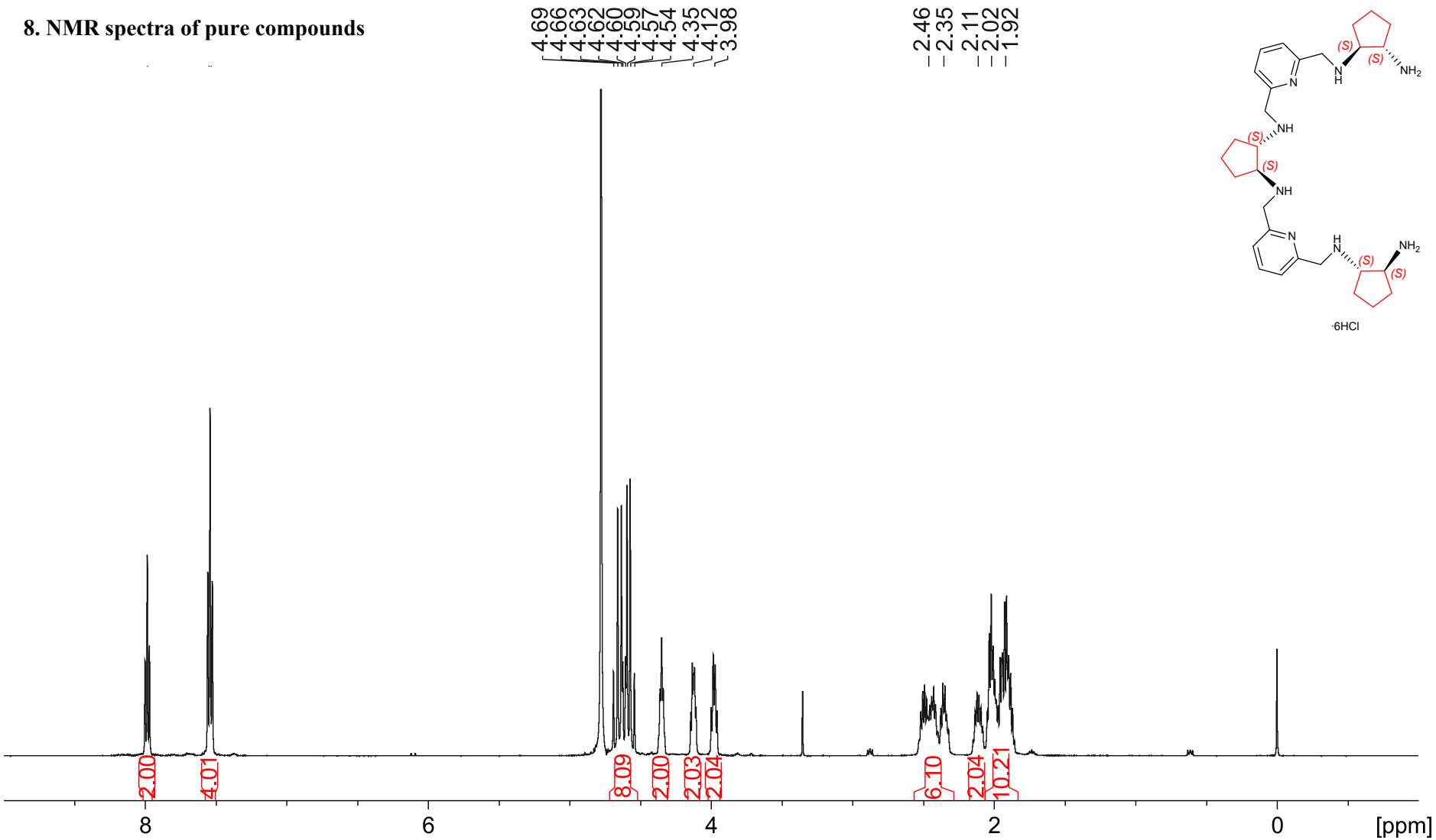

Supporting figure S10a. ^{1}H NMR spectrum (D_2O, DSS, 500 MHz) of protonated salt **14***ssssss*·6HCl·4.5H_2O.

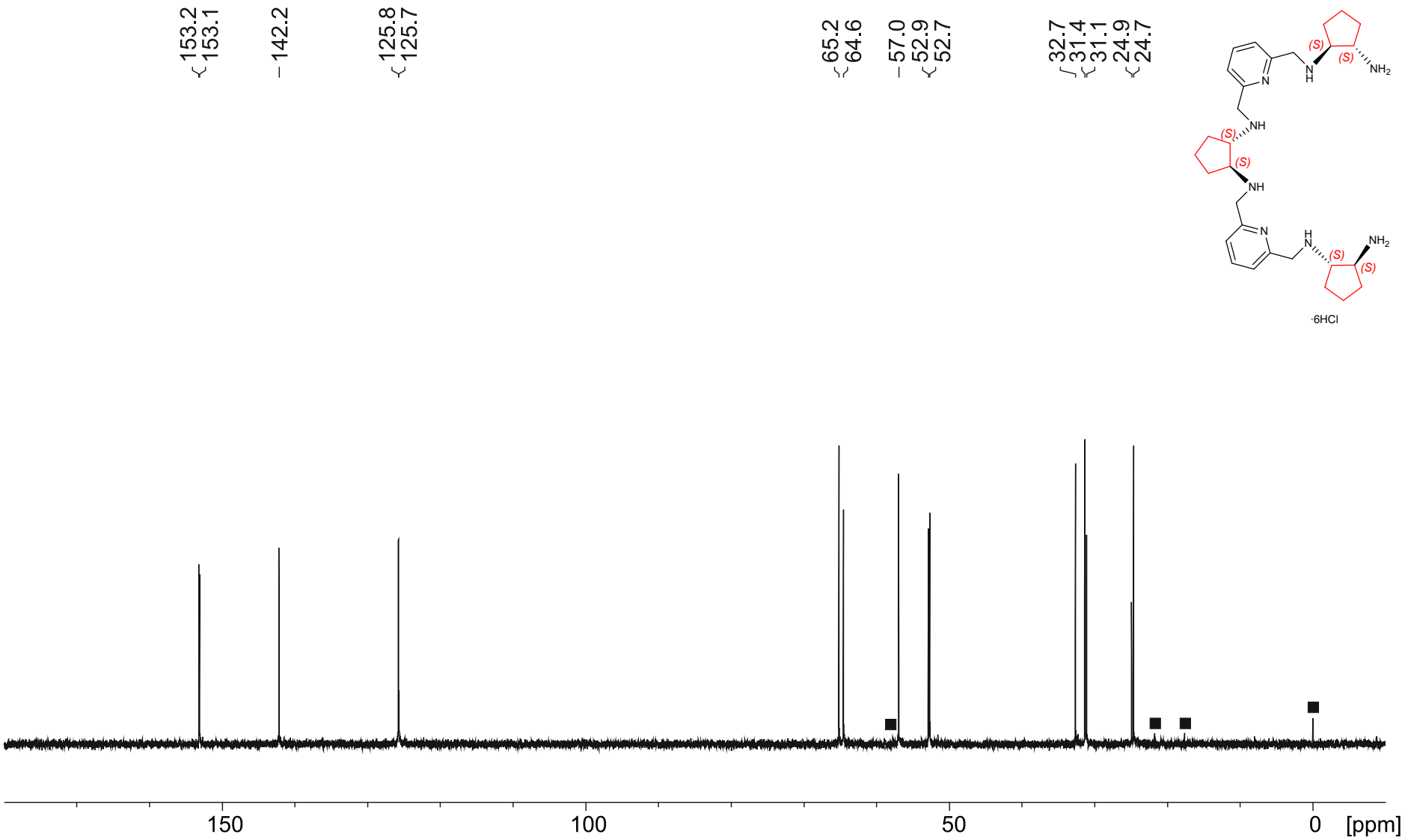

Supporting figure S10b. ^{13}C NMR spectrum (D_2O, DSS, 126 MHz) of protonated salt **14**$_{sssssss}$·6HCl·4.5H_2O.

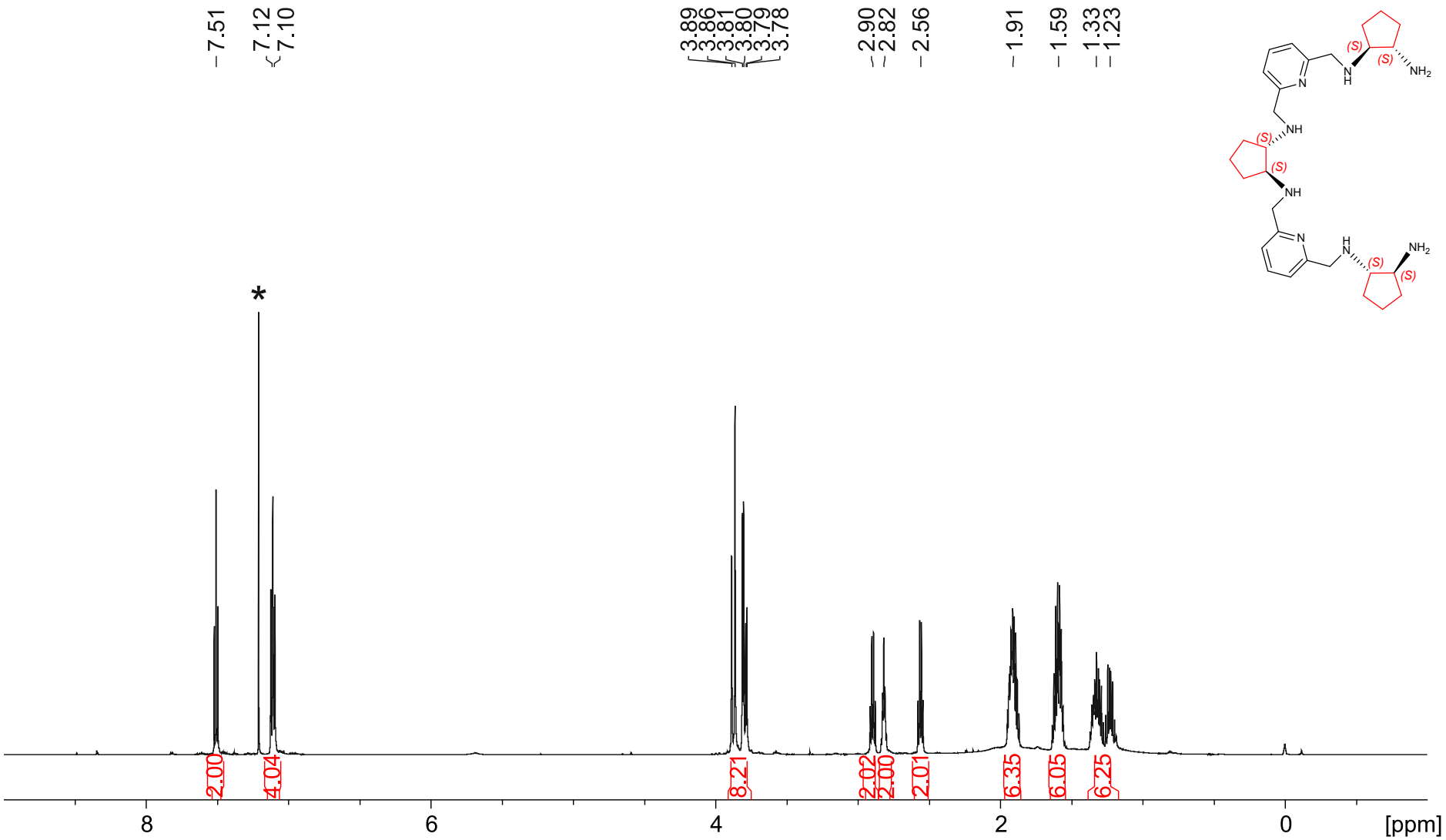

Supporting figure S11a. ^{1}H NMR spectrum ($CDCl_3$, 500 MHz) of amine **14**$_{SSSSSS}$·0.25CH_2Cl_2·0.5H_2O.

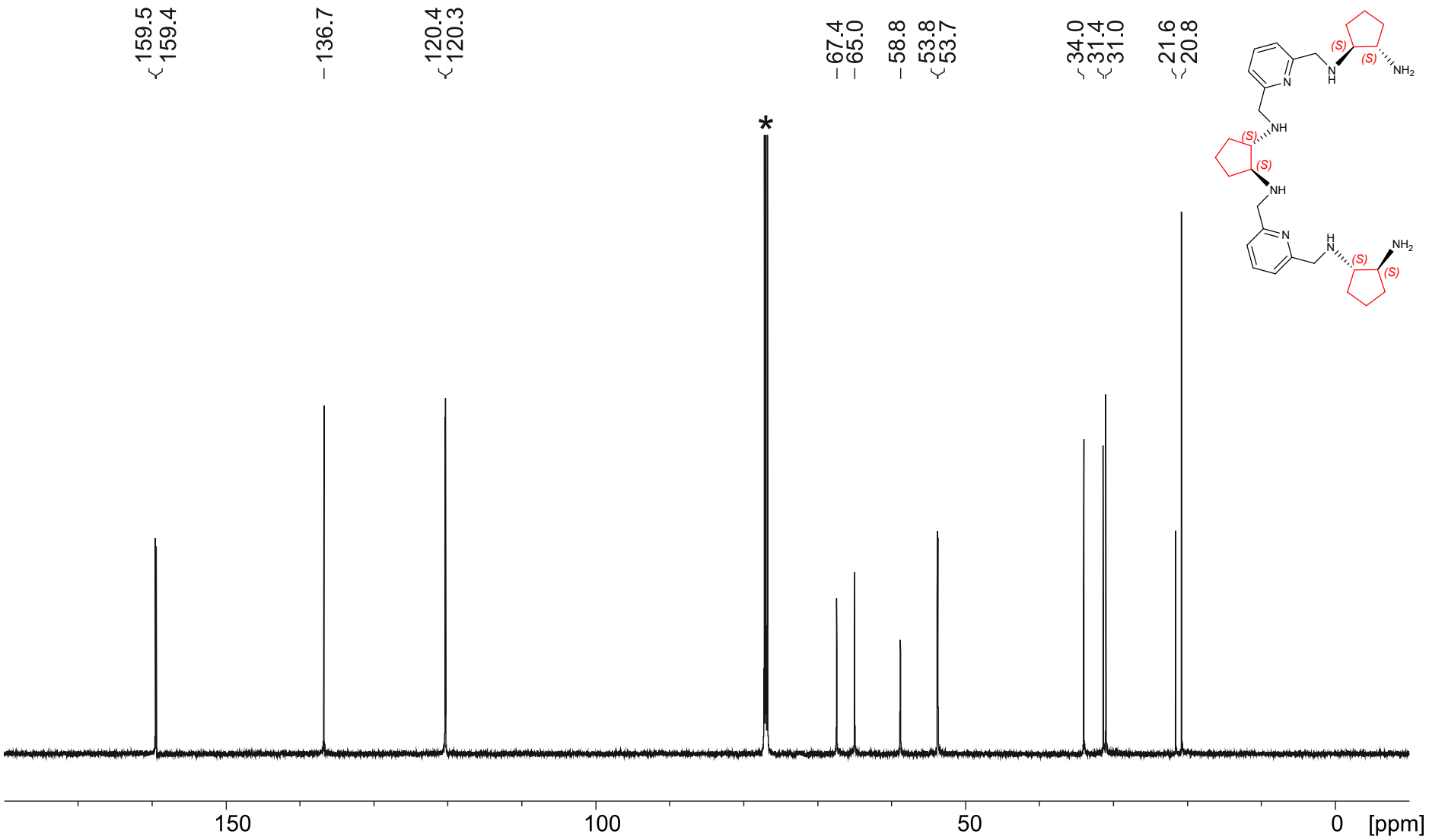

Supporting figure S11b. ^{13}C NMR spectrum ($CDCl_3$, 126 MHz) of amine **14**$_{sssssss}$·0.25CH_2Cl_2·0.5H_2O.

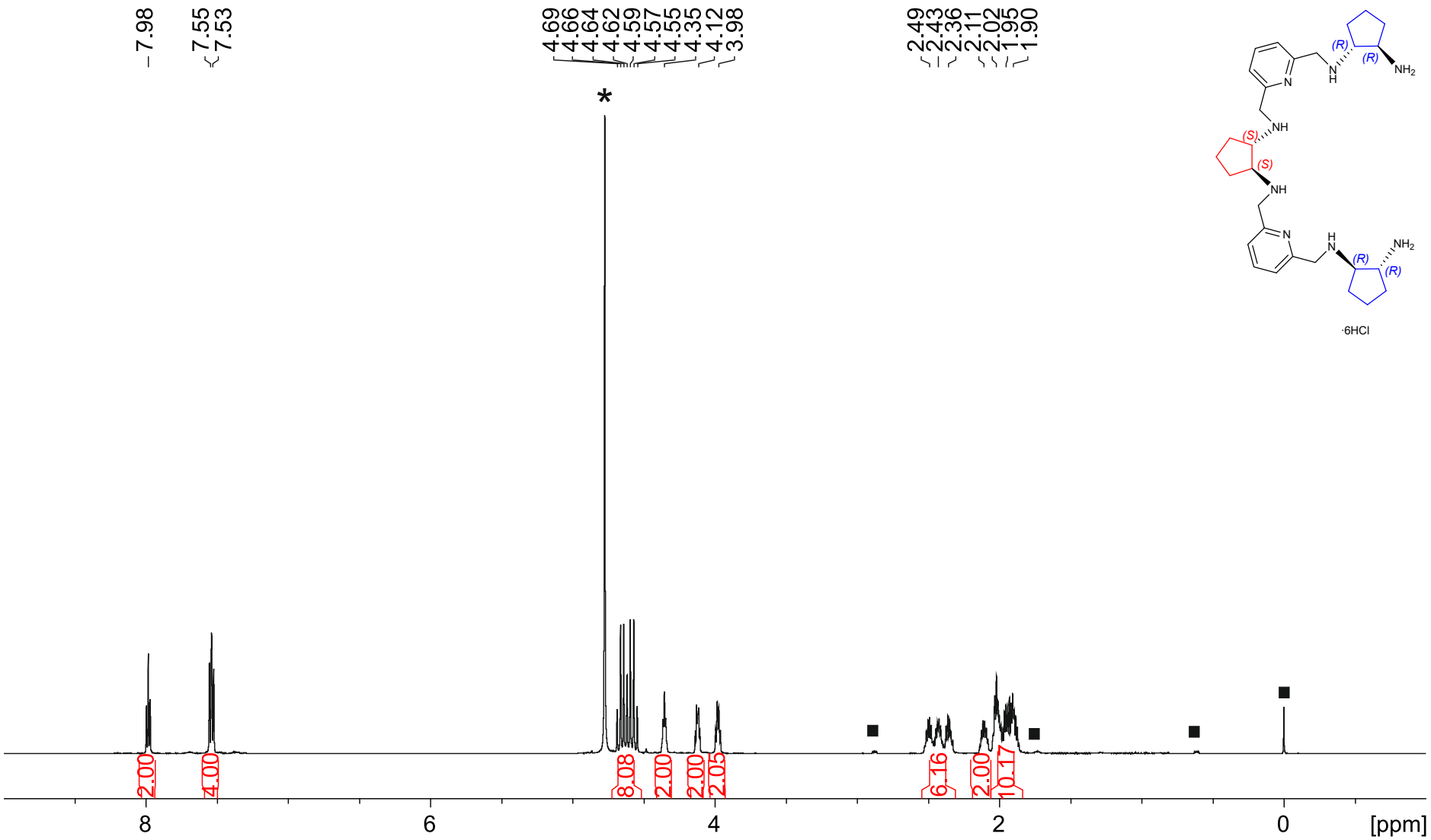

Supporting figure S12a. ^{1}H NMR spectrum (D_2O, DSS, 500 MHz) of protonated salt **14**$_{RRSSRR}$·6HCl·5.5H_2O.

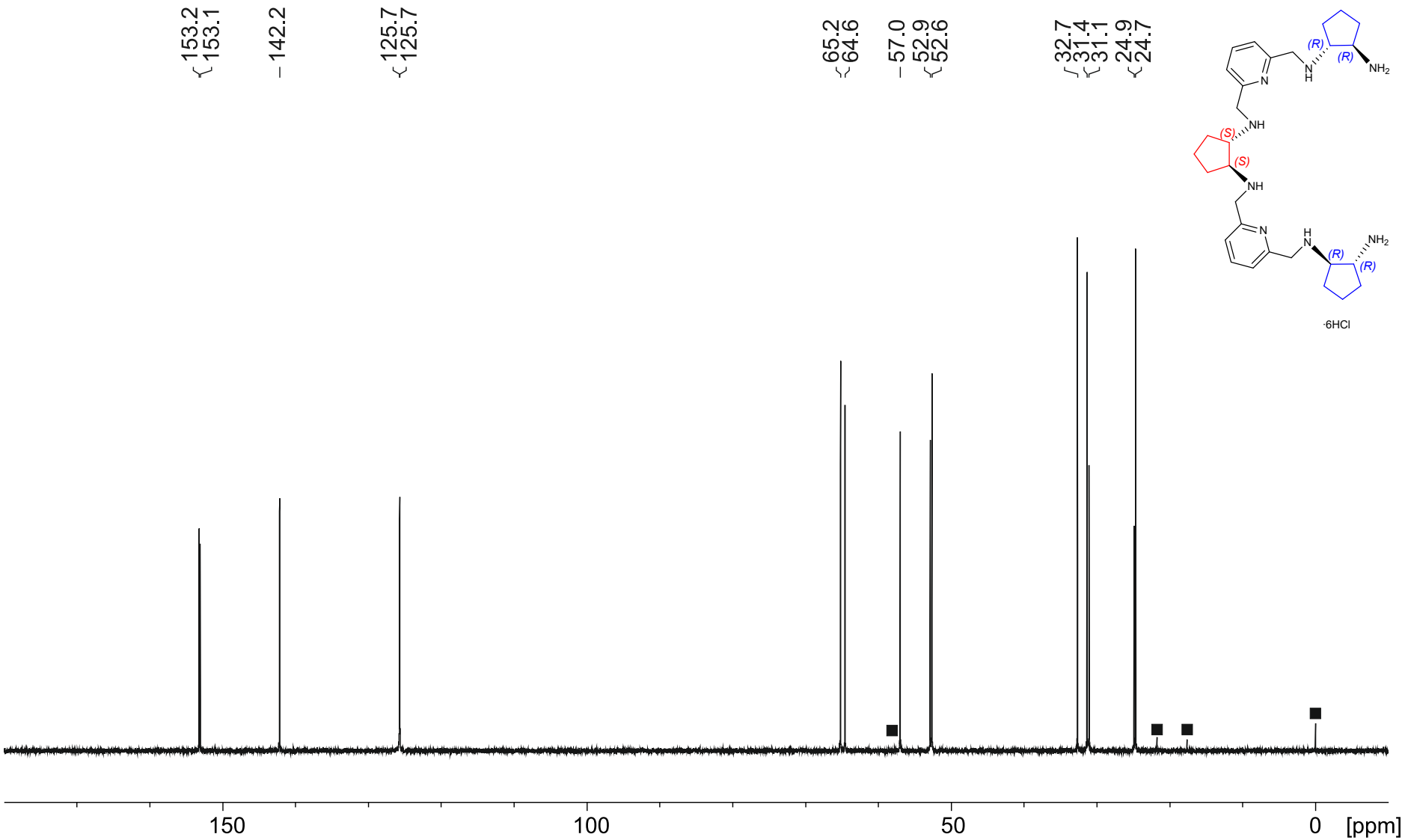

Supporting figure S12b. ^{13}C NMR spectrum (D_2O, DSS, 126 MHz) of protonated salt $\mathbf{14}_{RRSSRR}$·6HCl·5.5H_2O.

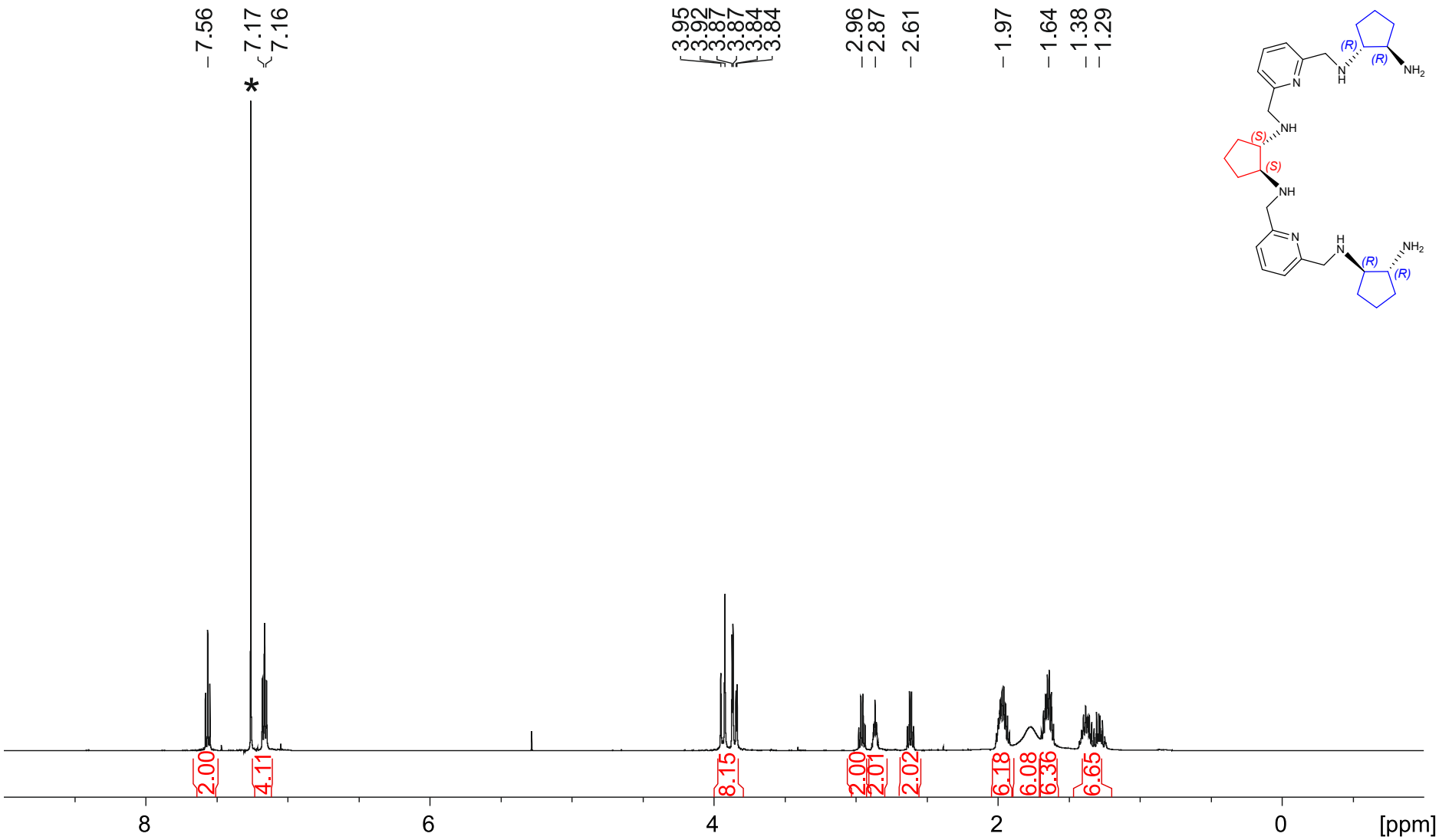

Supporting figure S13a. ^{1}H NMR spectrum ($CDCl_3$, 500 MHz) of amine $\mathbf{14}_{RRSSRR}\cdot 0.2CH_2Cl_2\cdot H_2O$.

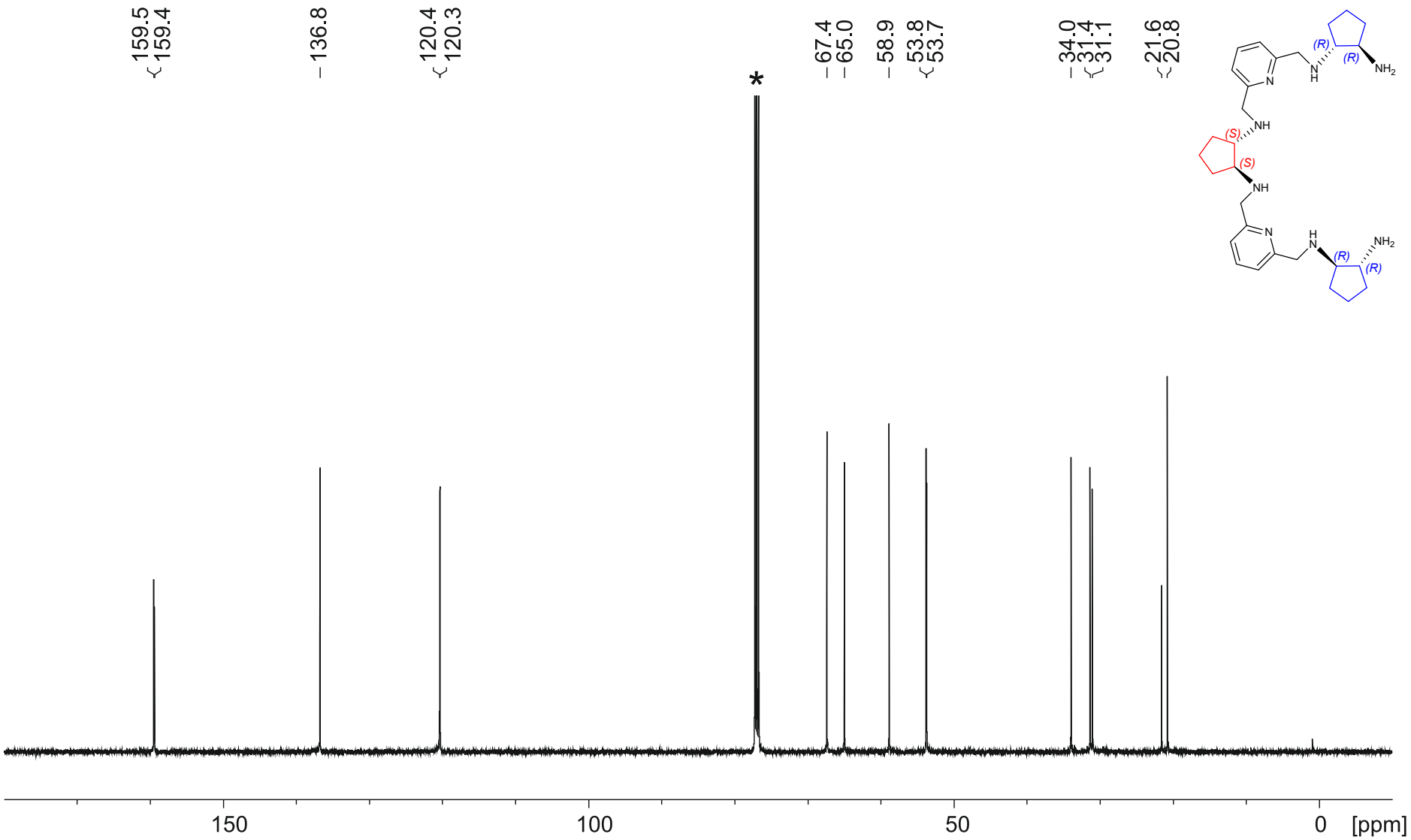

Supporting figure S13b. ^{13}C NMR spectrum ($CDCl_3$, 126 MHz) of amine $\mathbf{14}_{RRSSRR}\cdot 0.2CH_2Cl_2\cdot H_2O$.

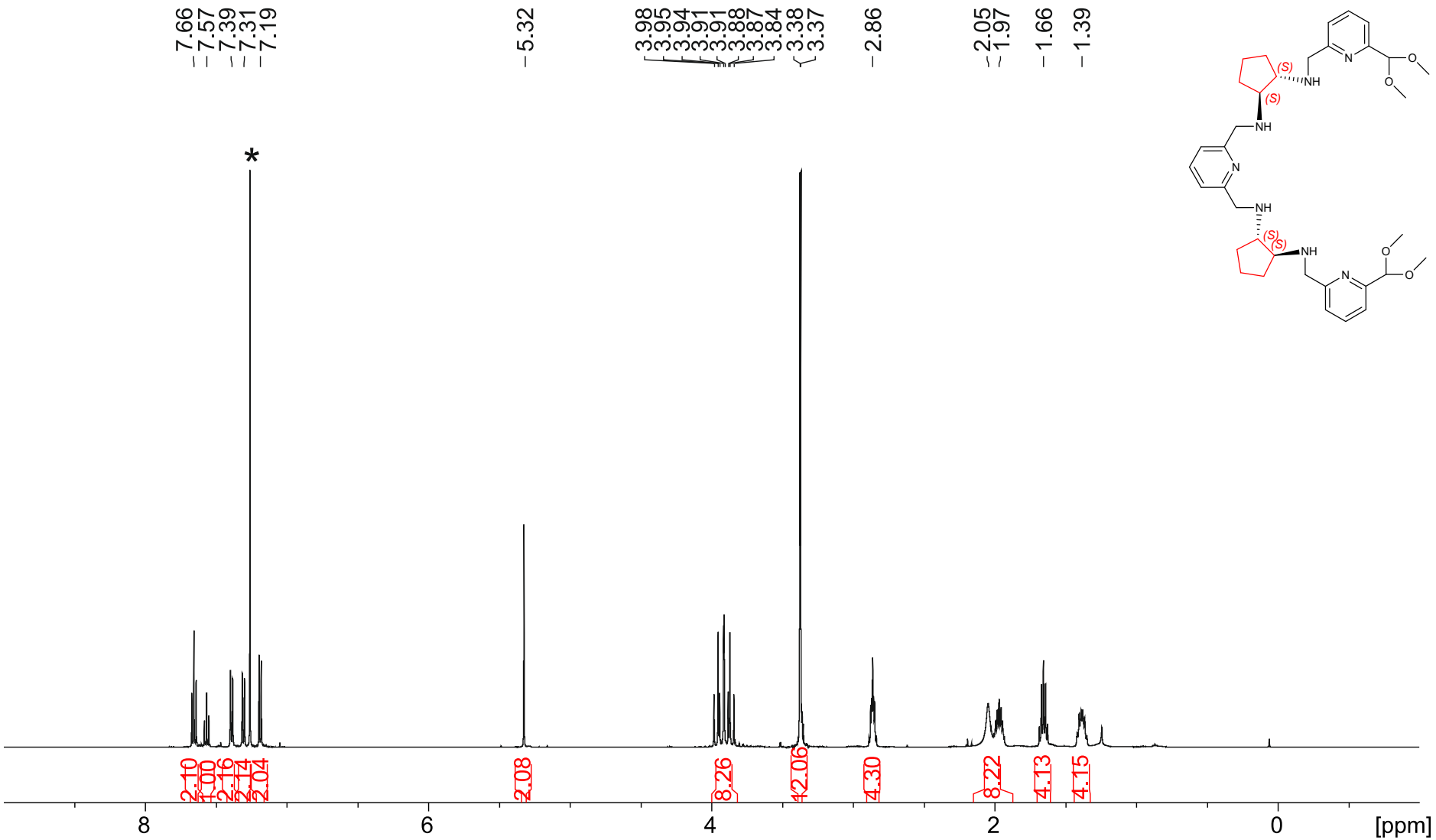

Supporting figure S14a. ^{1}H NMR spectrum ($CDCl_3$, 500 MHz) of diprotected dialdehyde **15**$_{SSSS}$·0.2$CHCl_3$·2.5H_2O.

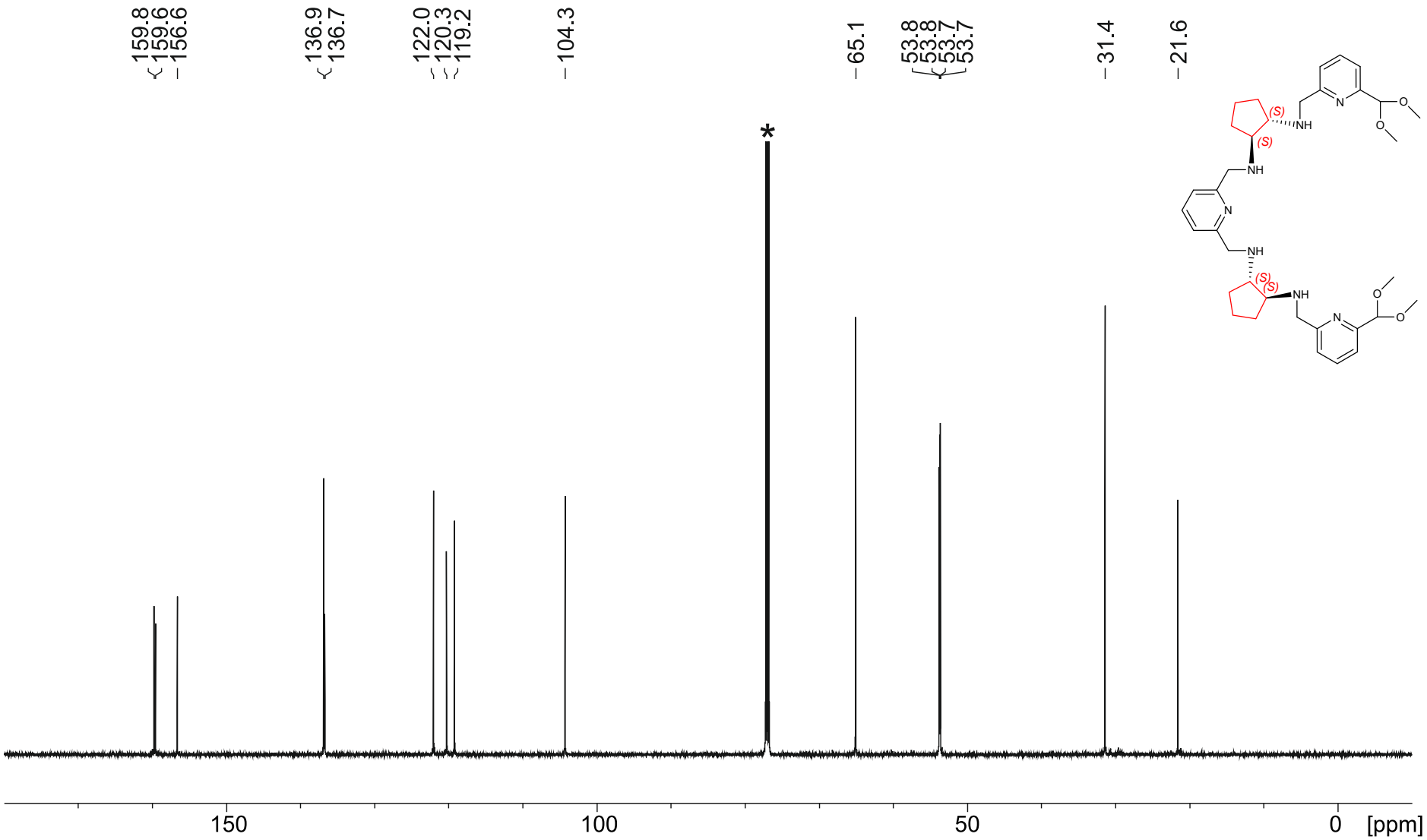

Supporting figure S14b. ^{13}C NMR spectrum ($CDCl_3$, 126 MHz) of diprotected dialdehyde **15**$_{SSSS}$·0.2$CHCl_3$·2.5H_2O.

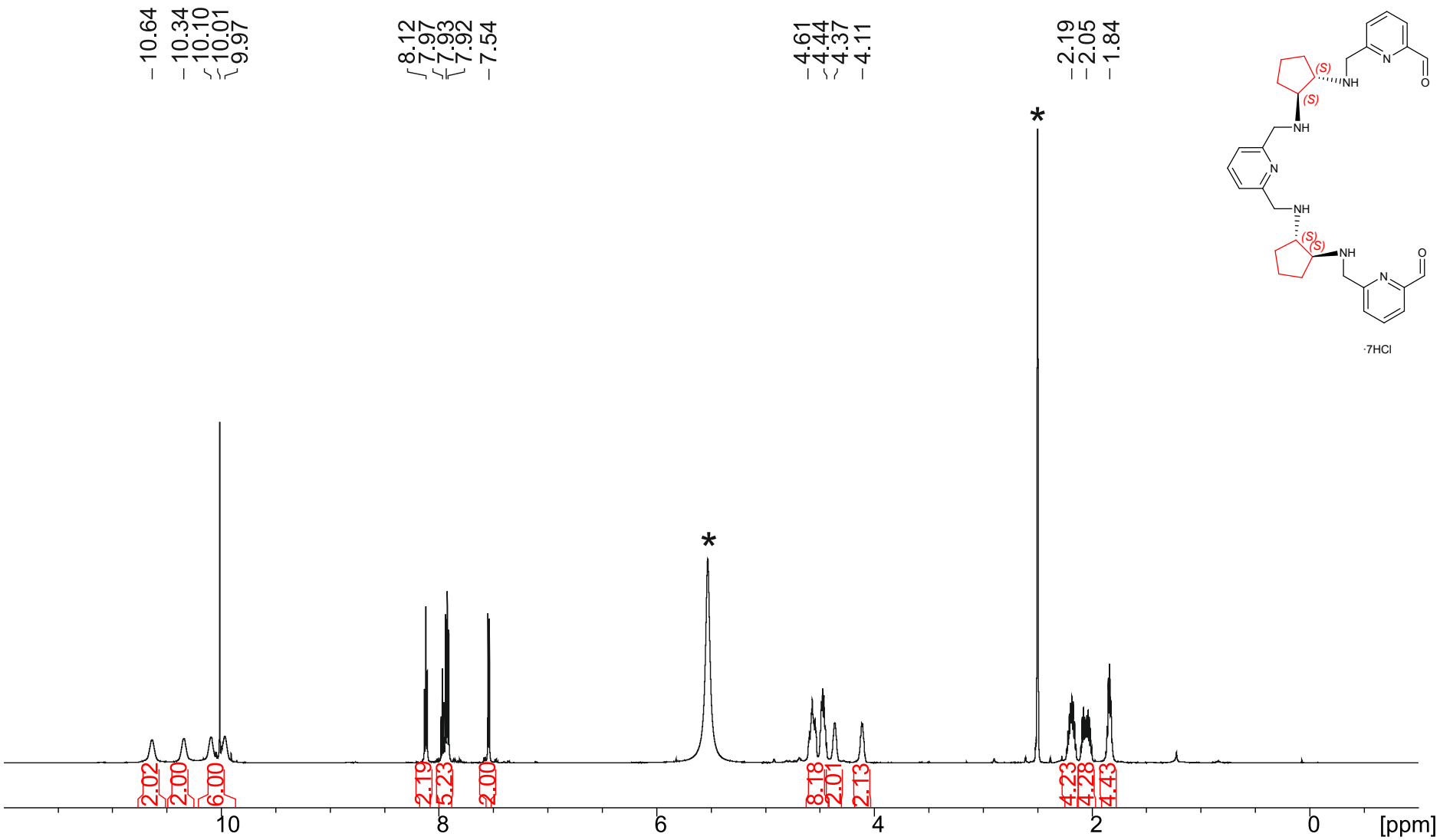

Supporting figure S15a. ^{1}H NMR spectrum (DMSO-d_6, 500 MHz) of hydrochloride salt of dialdehyde **16**$_{SSSS}$·7HCl·0.25H_2O.

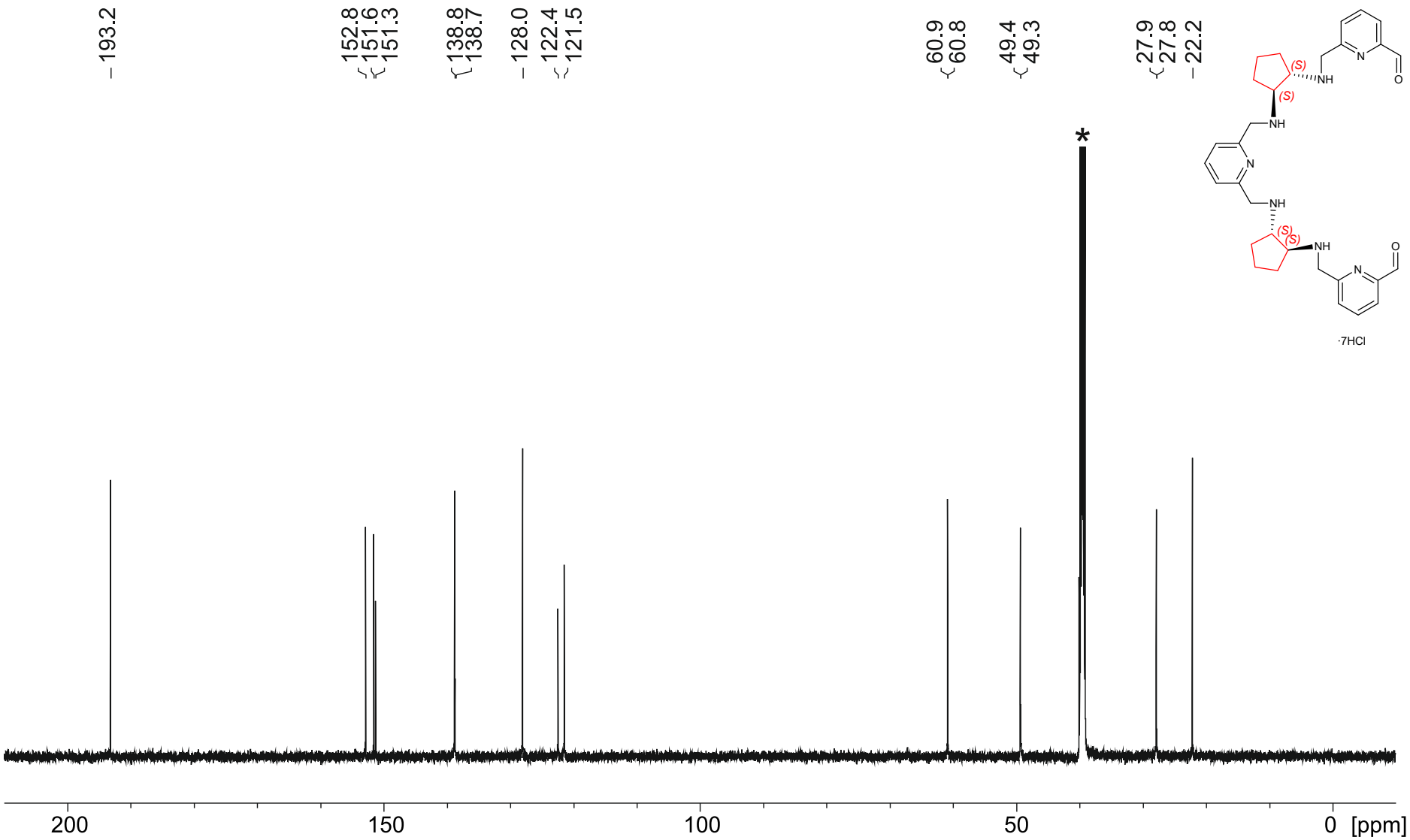

Supporting figure S15b. ^{13}C NMR spectrum (DMSO-d_6, 126 MHz) of hydrochloride salt of dialdehyde **16**$_{SSSS}$·7HCl·0.25H_2O.

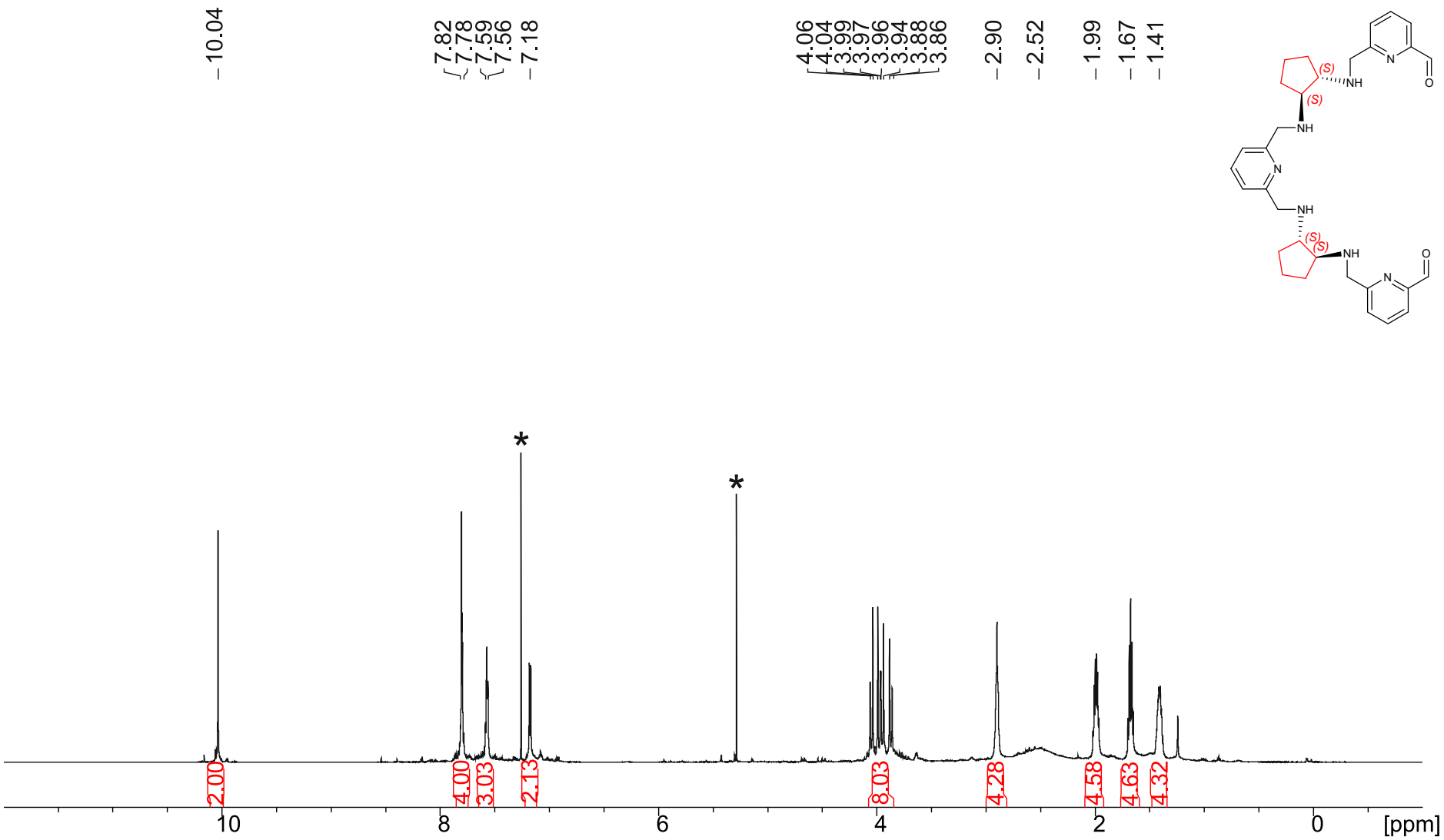

Supporting figure S16a. ^{1}H NMR spectrum ($CDCl_3$, 500 MHz) of dialdehyde **16**$_{SSSS}$·CH_2Cl_2.

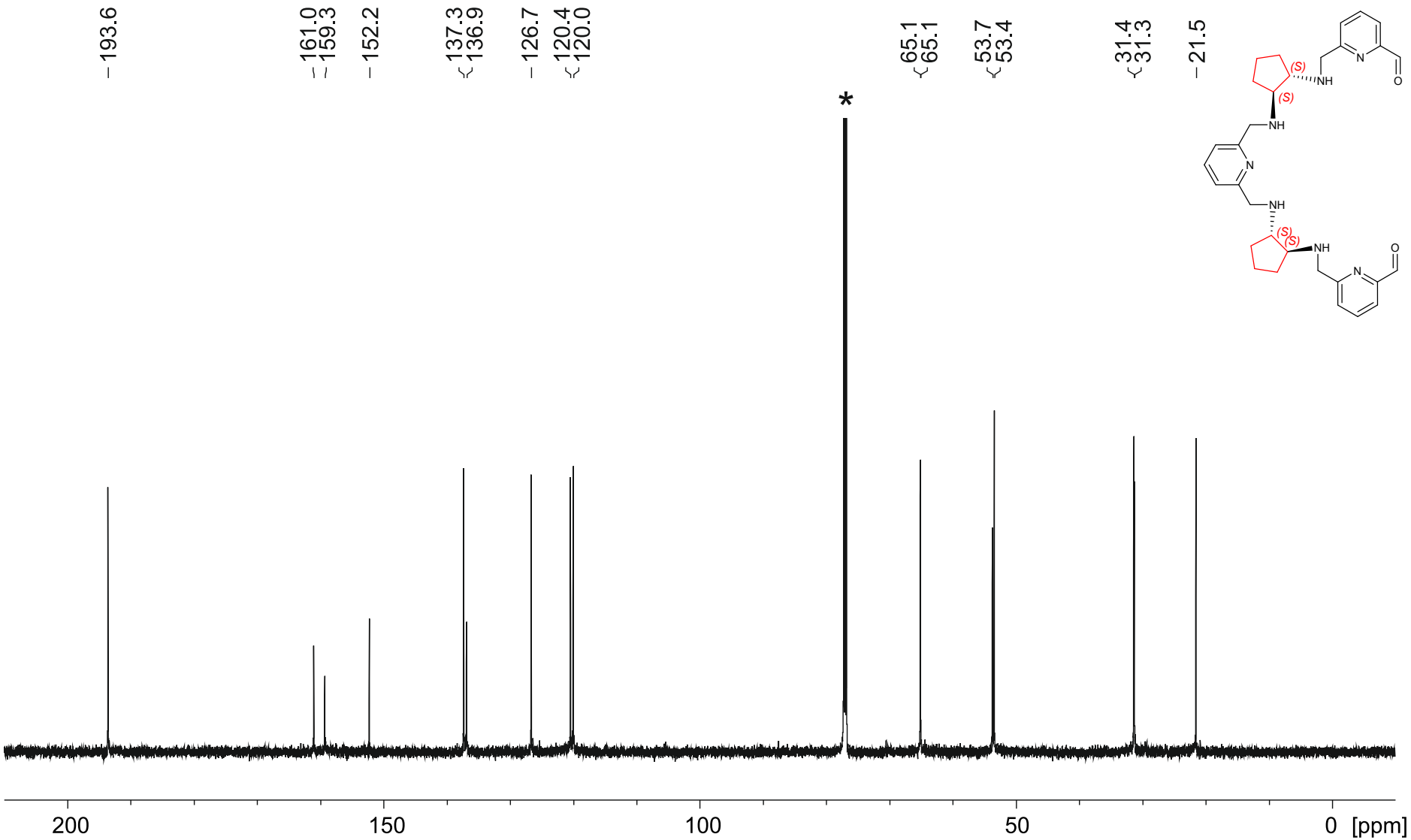

Supporting figure S16b. ^{13}C NMR spectrum ($CDCl_3$, 126 MHz) of dialdehyde **16**$_{SSSS}$·CH_2Cl_2.

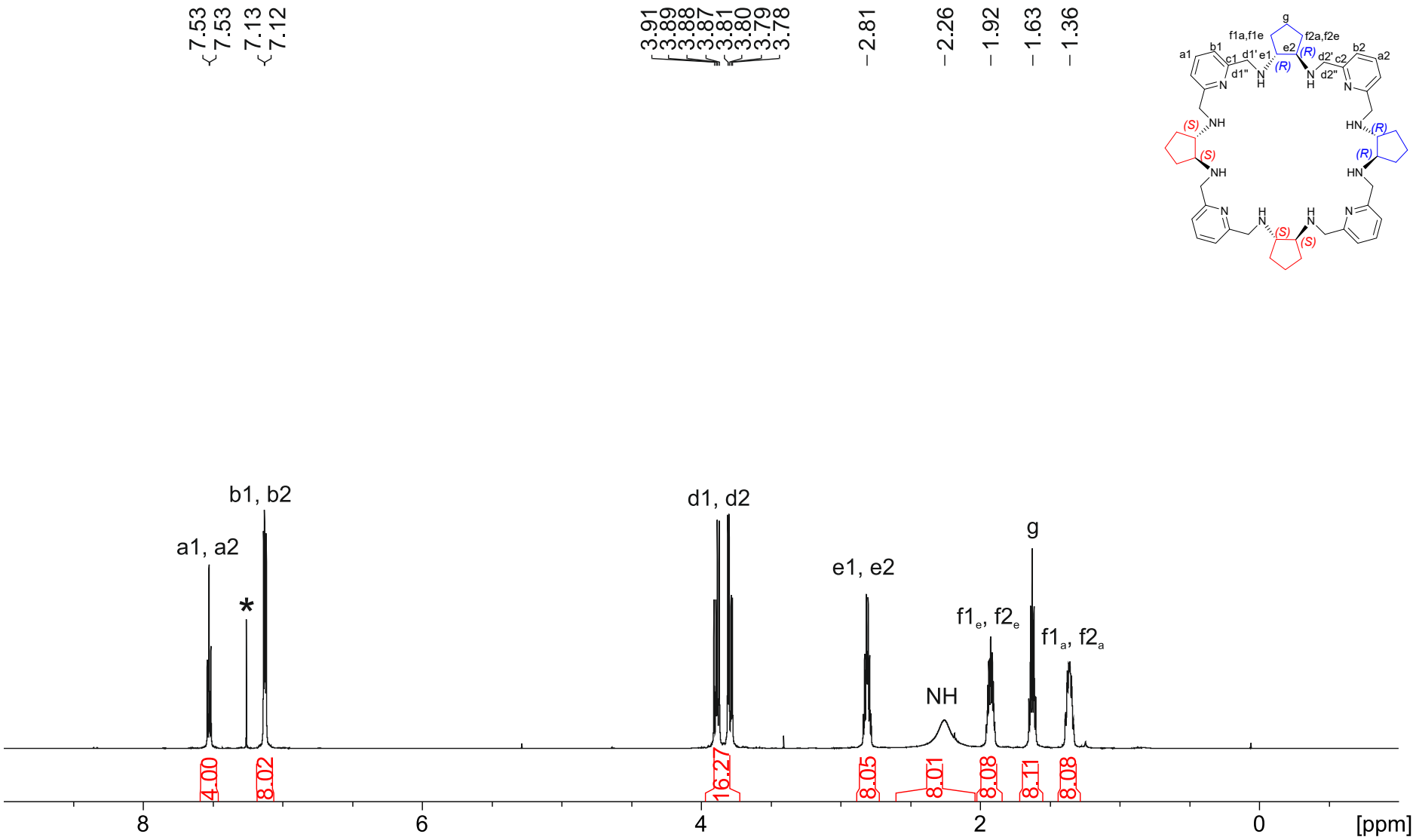

Supporting figure S17a. ^{1}H NMR spectrum (500 MHz, $CDCl_3$) of macrocyclic amine **3**·H_2O.

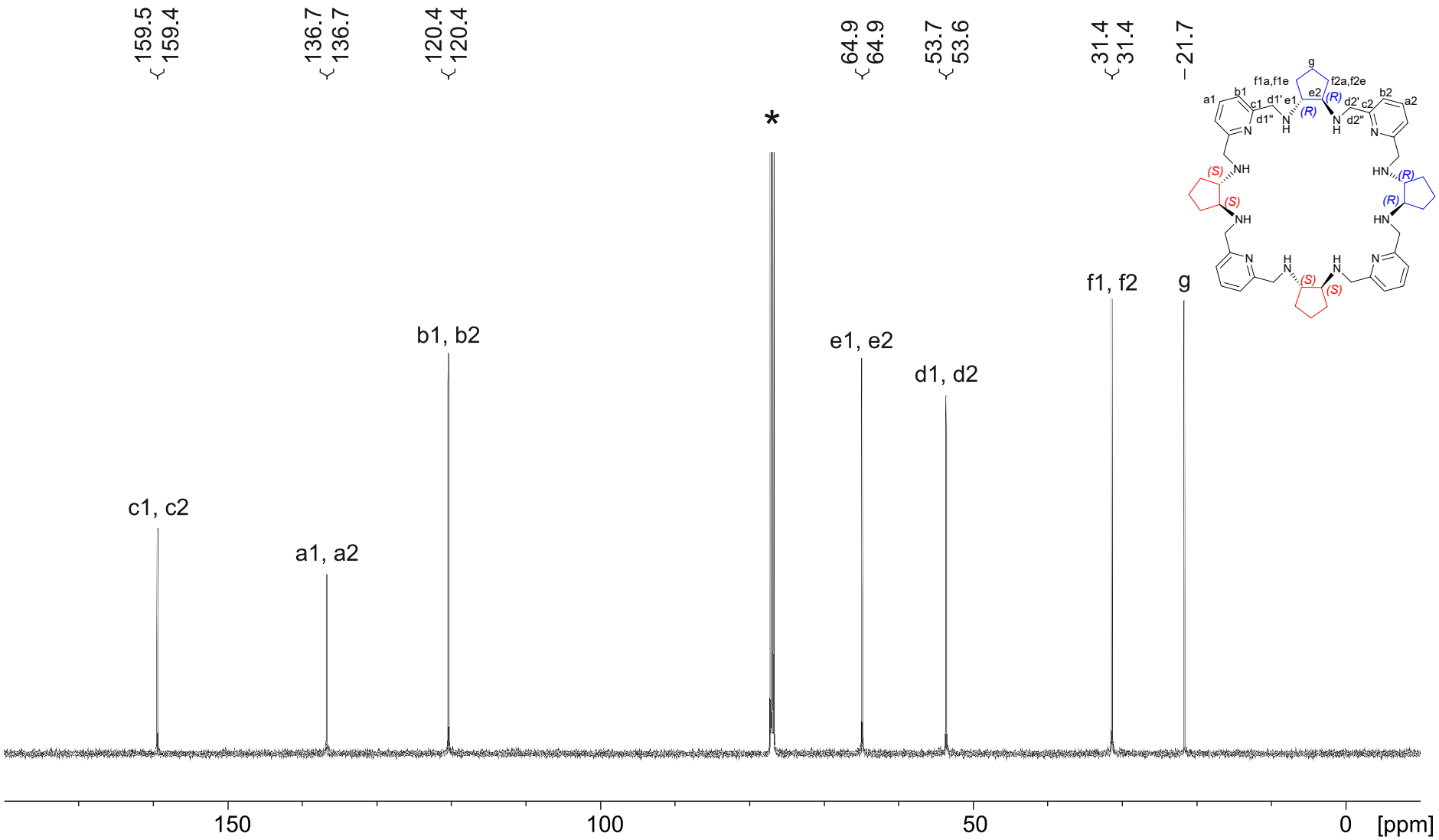

Supporting figure S17b. $^{13}C\ \{^{1}H\}$ NMR spectrum (126 MHz, $CDCl_3$) of macrocyclic amine **3**·H_2O.

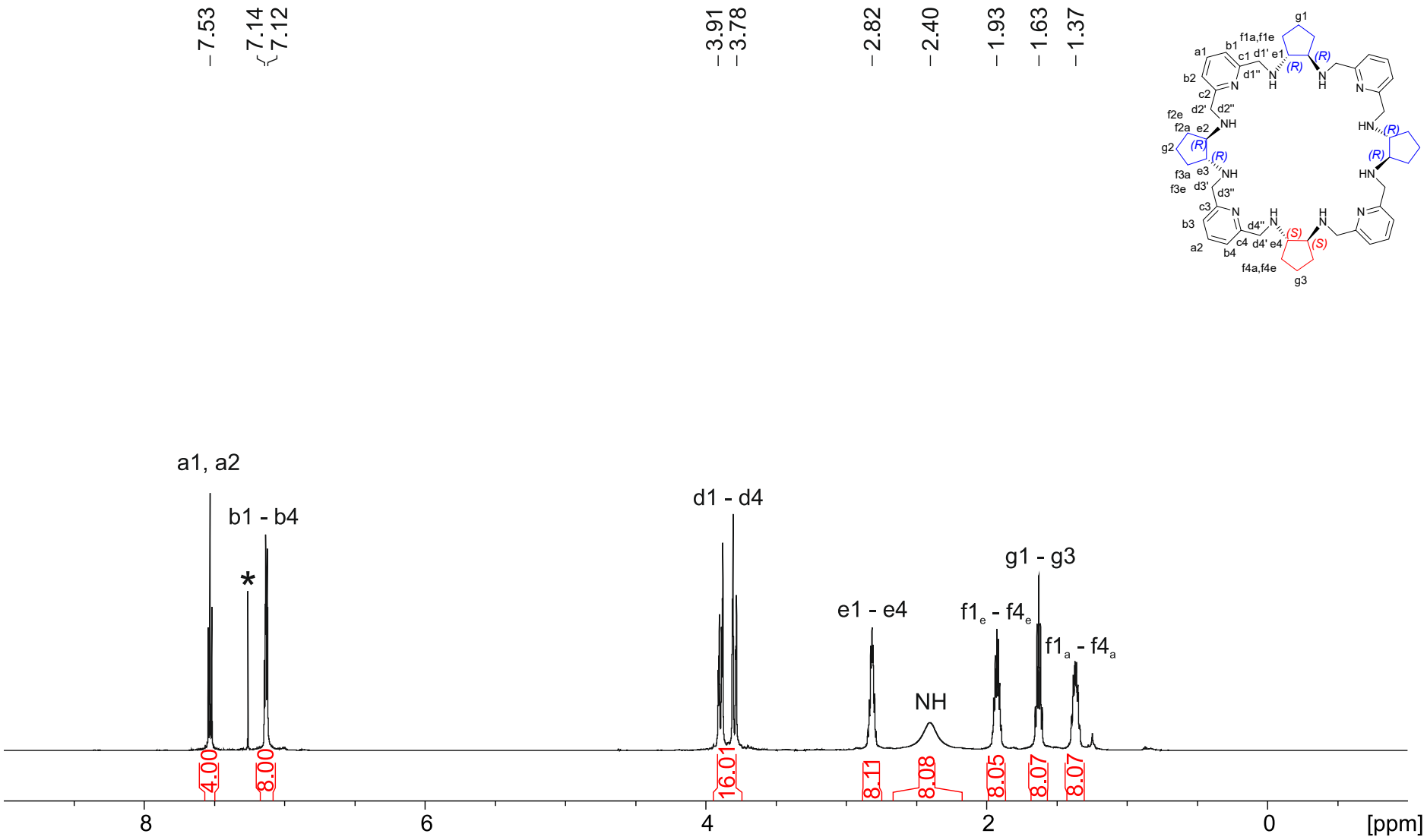

Supporting figure S18a. ^{1}H NMR spectrum (500 MHz, $CDCl_3$) of macrocyclic amine $\mathbf{4}_{SSSSSSRR}\cdot 1.25H_2O$.

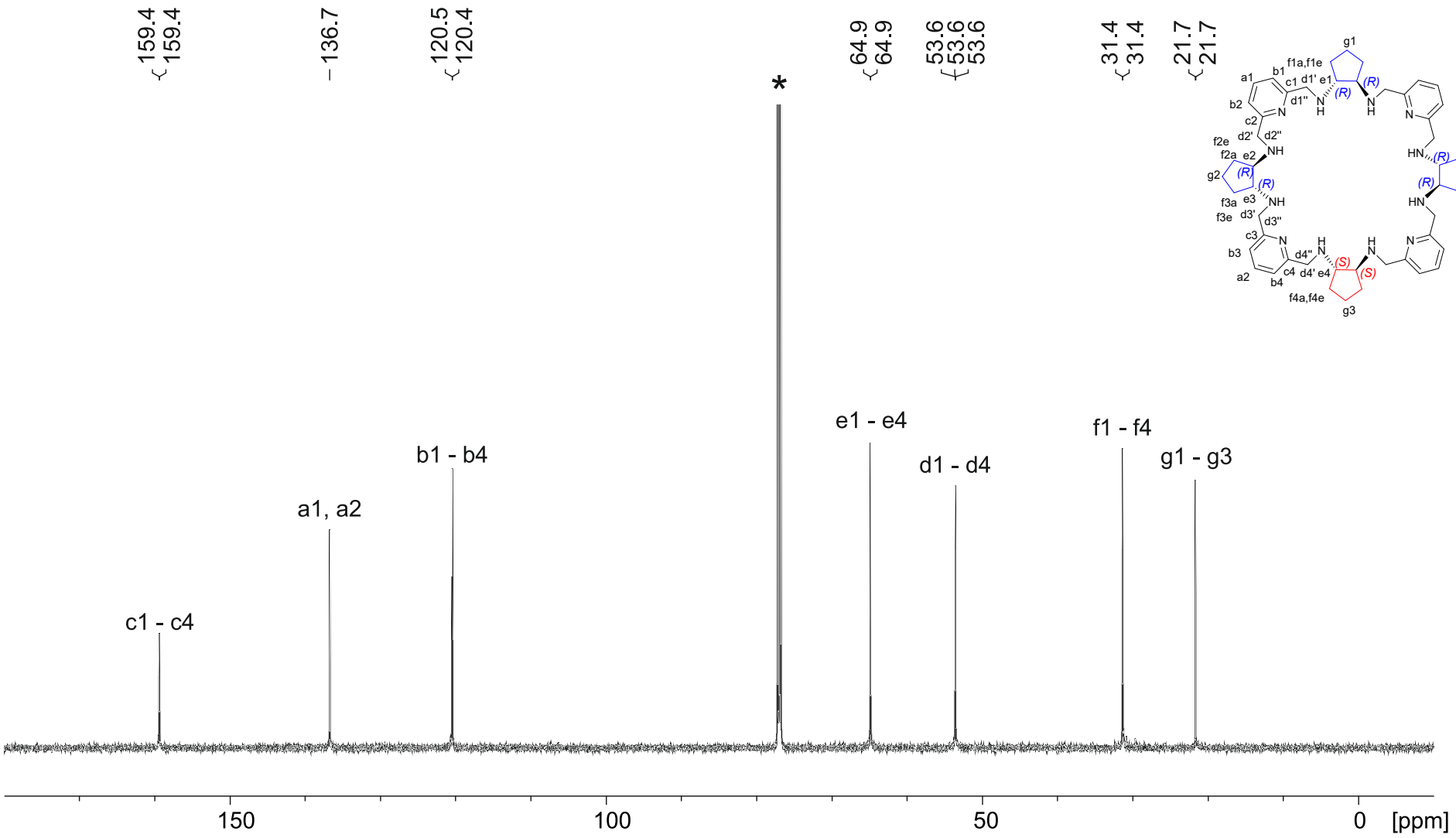

Supporting figure S18b. $^{13}C\ \{^{1}H\}$ NMR spectrum (126 MHz, $CDCl_3$) of macrocyclic amine $\mathbf{4}_{SSSSSSRR}\cdot 1.25H_2O$.

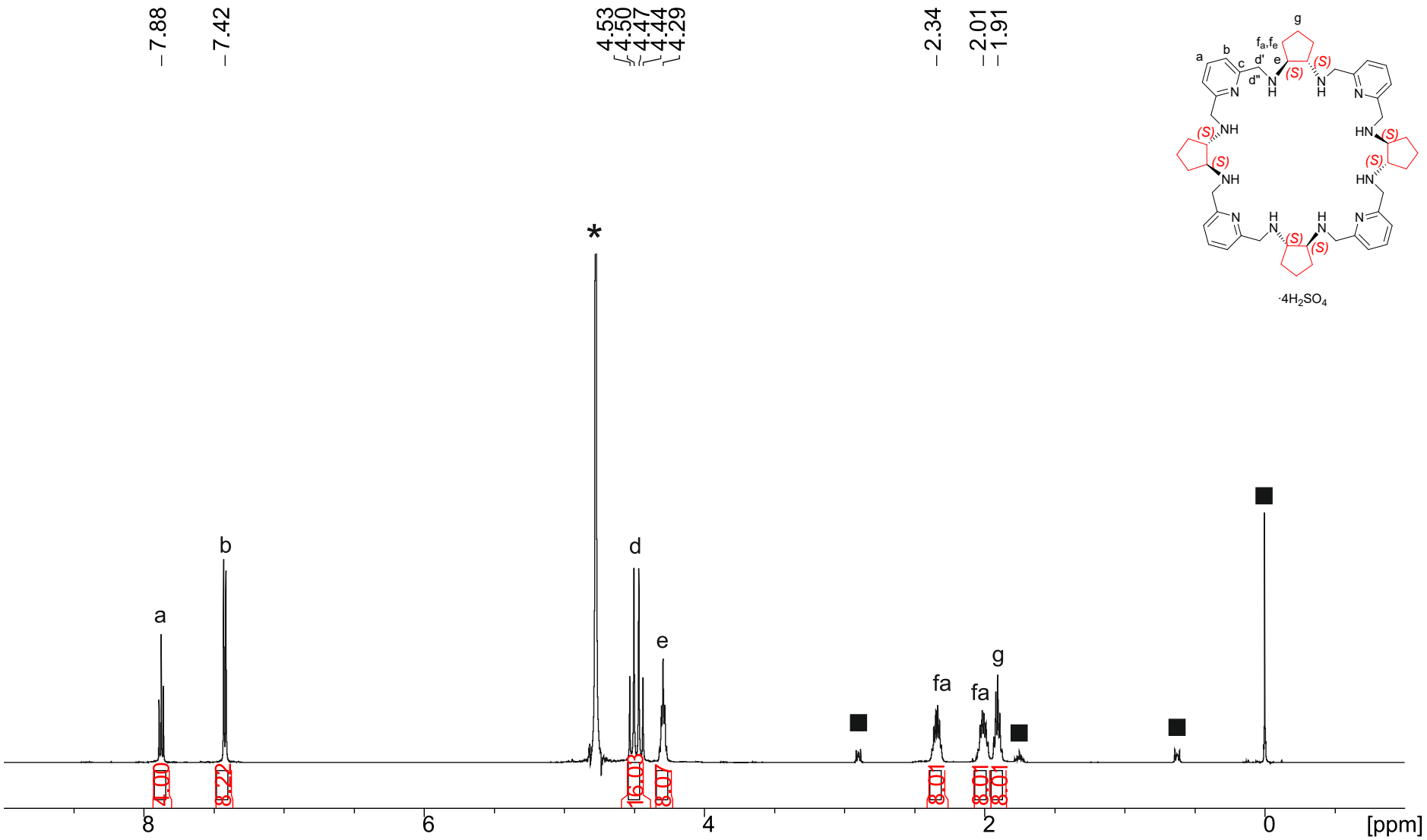

Supporting figure S19a. ^{1}H NMR spectrum (500 MHz, D_2O) of protonated with sulfuric acid macrocyclic amine [(**1***sssssssss*)H_8]$(HSO_4)_4(SO_4)_2\cdot 16H_2O$.

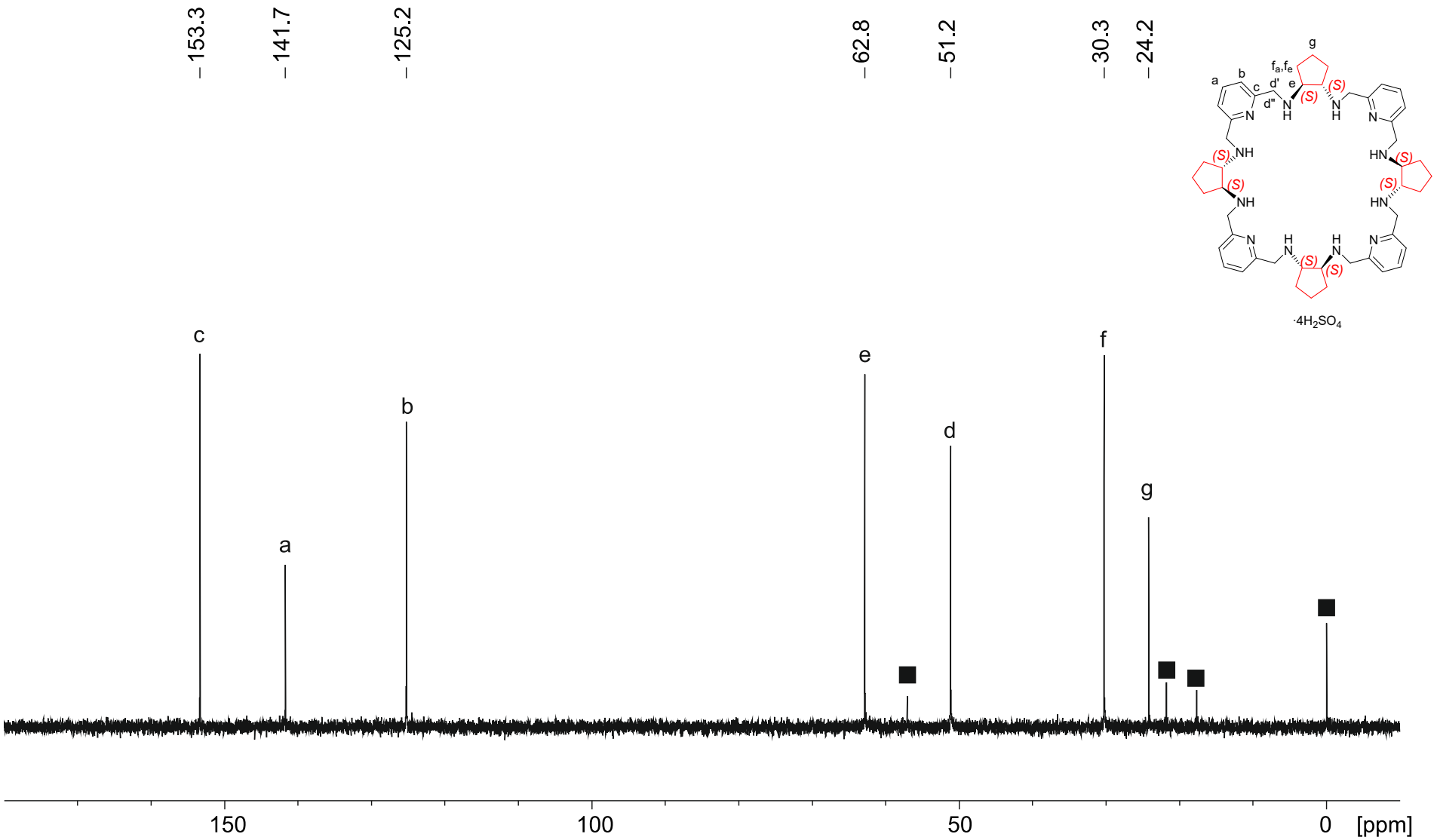

Supporting figure S19b. ^{13}C NMR spectrum (126 MHz, D_2O) of protonated with sulfuric acid macrocyclic amine [(**1***ssssssss*)H_8]$(HSO_4)_4(SO_4)_2 \cdot 16H_2O$.

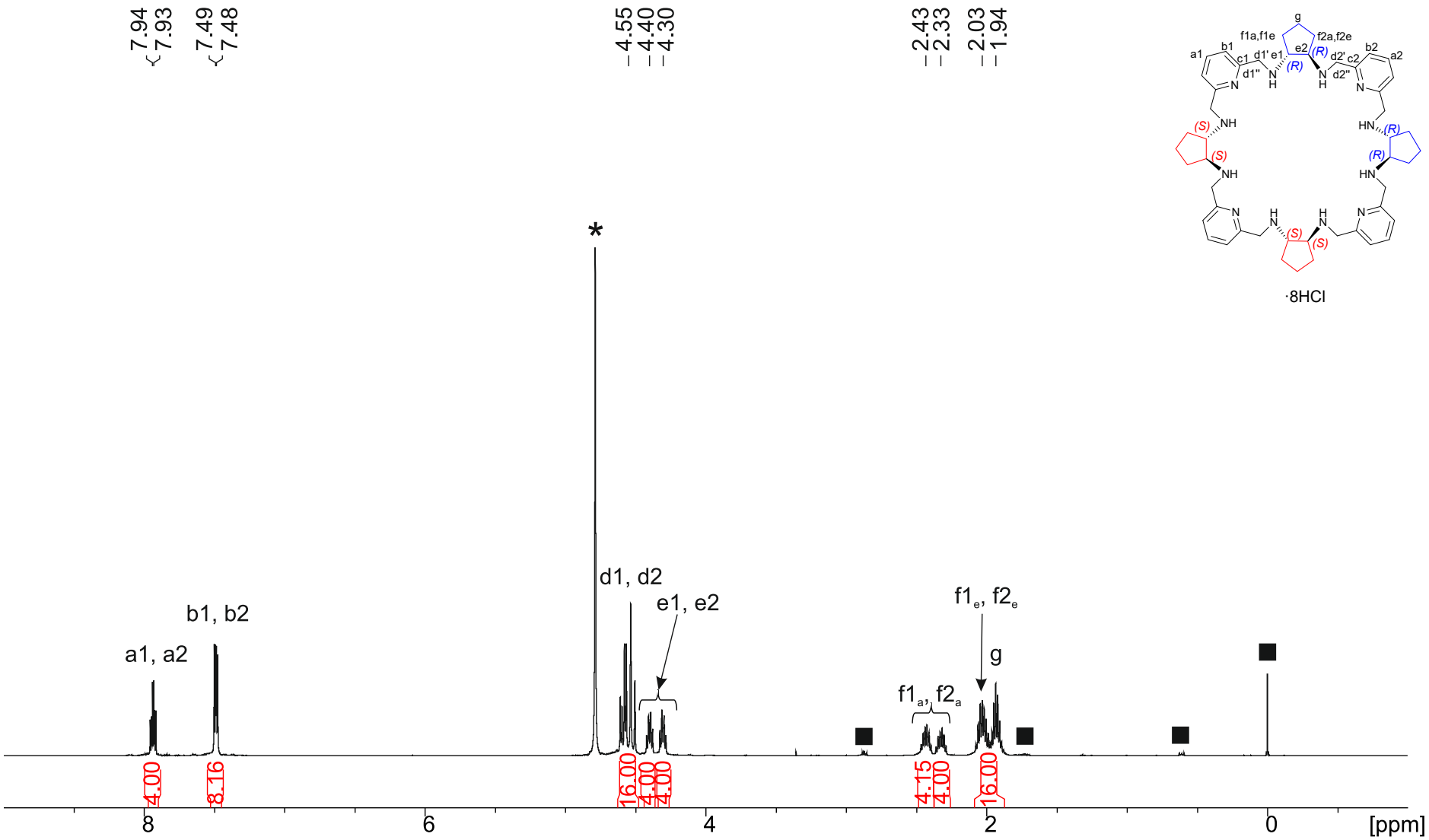

Supporting figure S20a. ^{1}H NMR spectrum (500 MHz, D_2O) of protonated macrocyclic amine [(**3**)H_8]Cl_8·6H_2O.

.

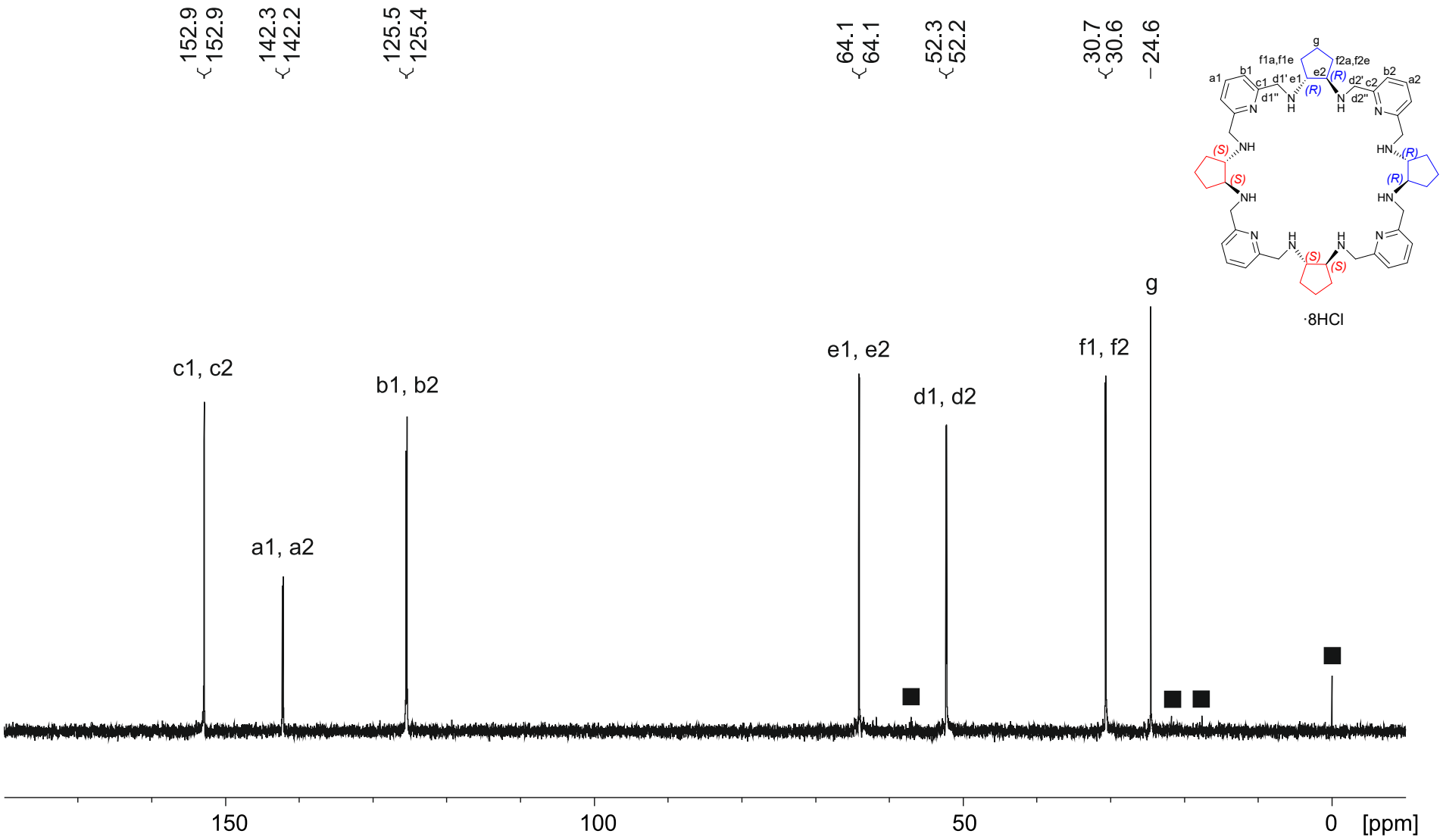

Supporting figure S20b. $^{13}C\ \{^{1}H\}$ NMR spectrum (126 MHz, D_2O) of protonated macrocyclic amine [(**3**)H_8]$Cl_8 \cdot 6H_2O$.

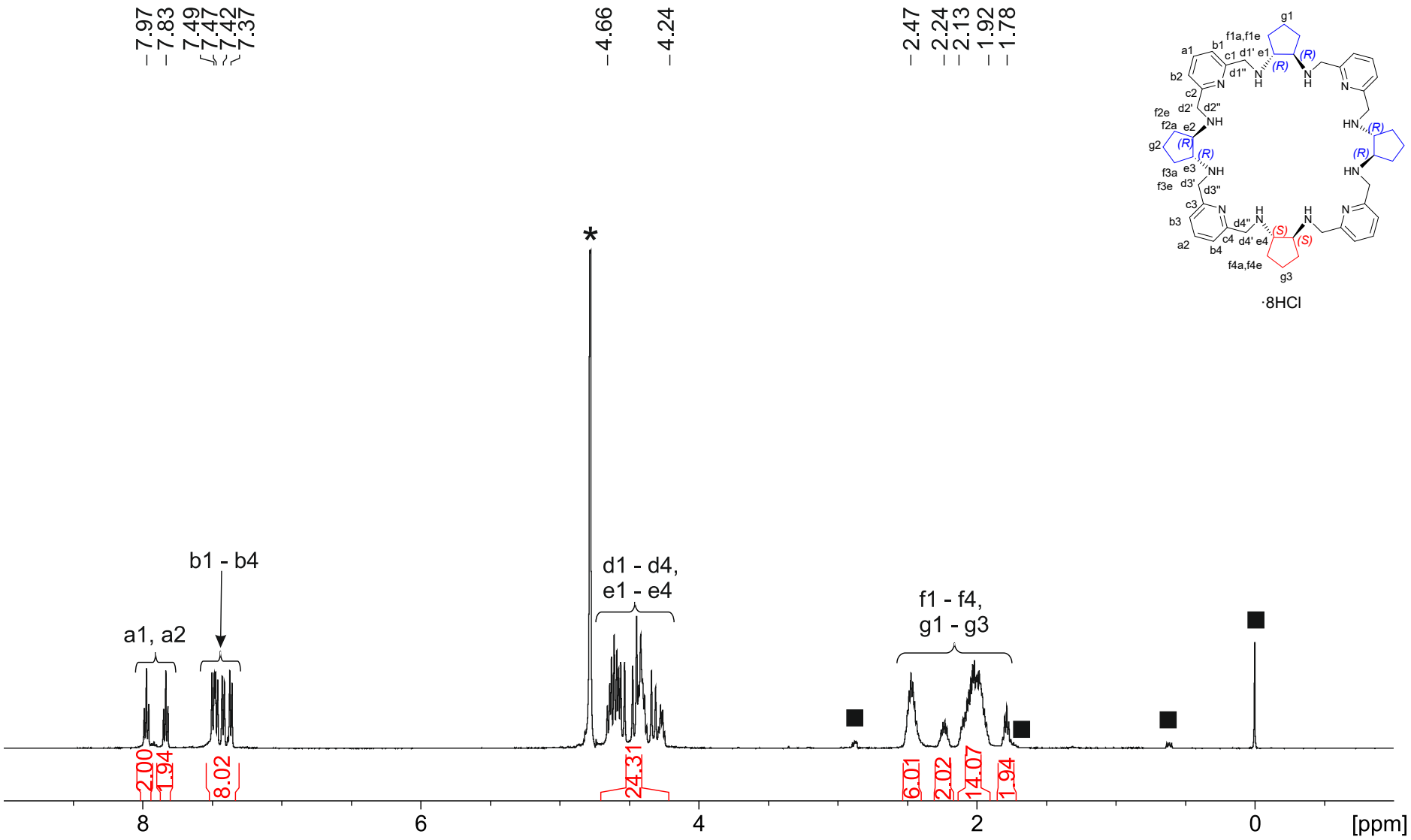

Supporting figure S21a. ^{1}H NMR spectrum (500 MHz, D_2O) of protonated macrocyclic amine $[(\mathbf{4}_{RRRRRRSS})H_8]Cl_8 \cdot 3.5H_2O$.

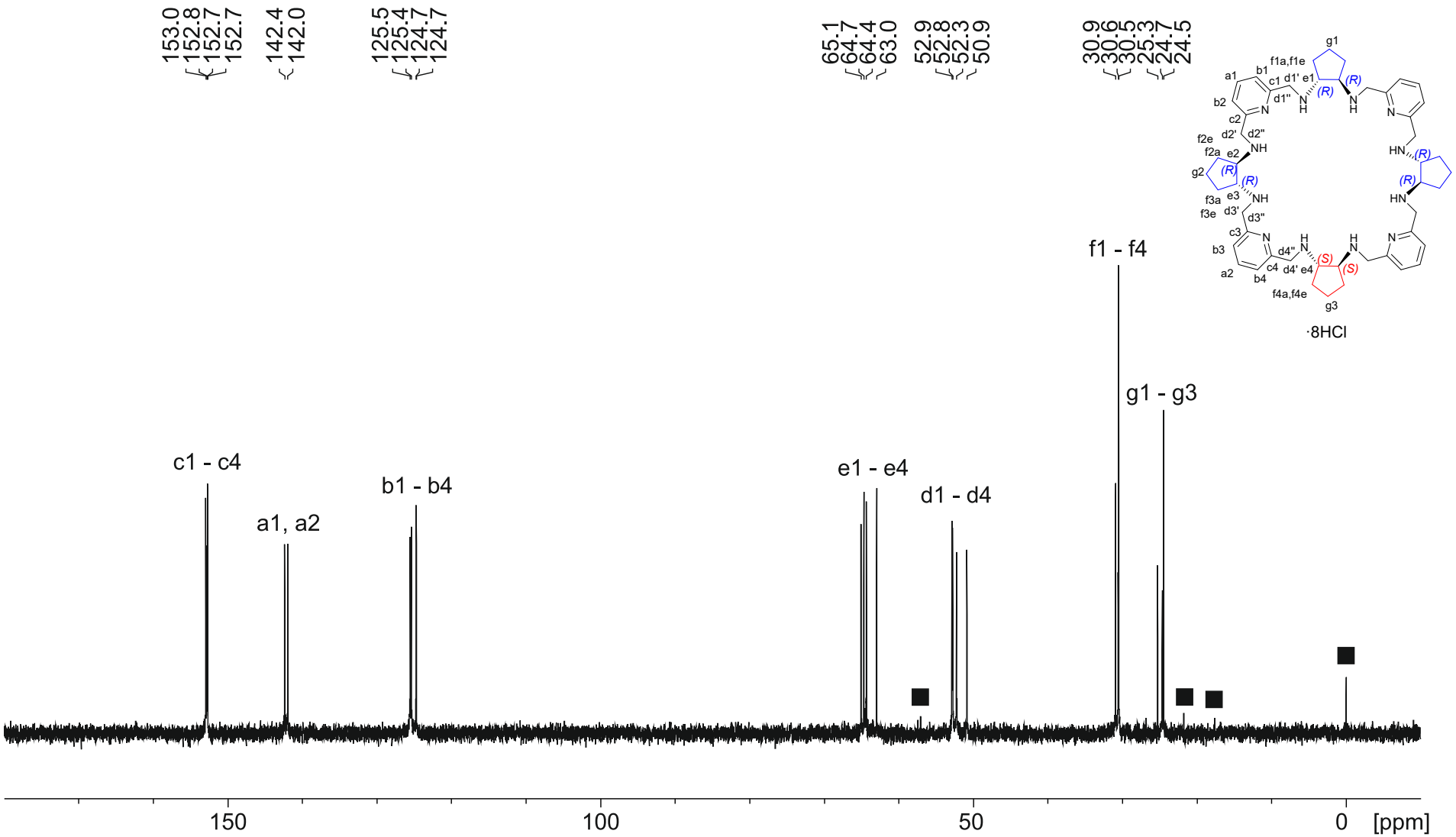

Supporting figure S21b. ^{13}C {^{1}H} NMR spectrum (126 MHz, D_2O) of protonated macrocyclic amine [(**4**$_{RRRRRRSS}$)H_8]Cl_8·3.5H_2O.

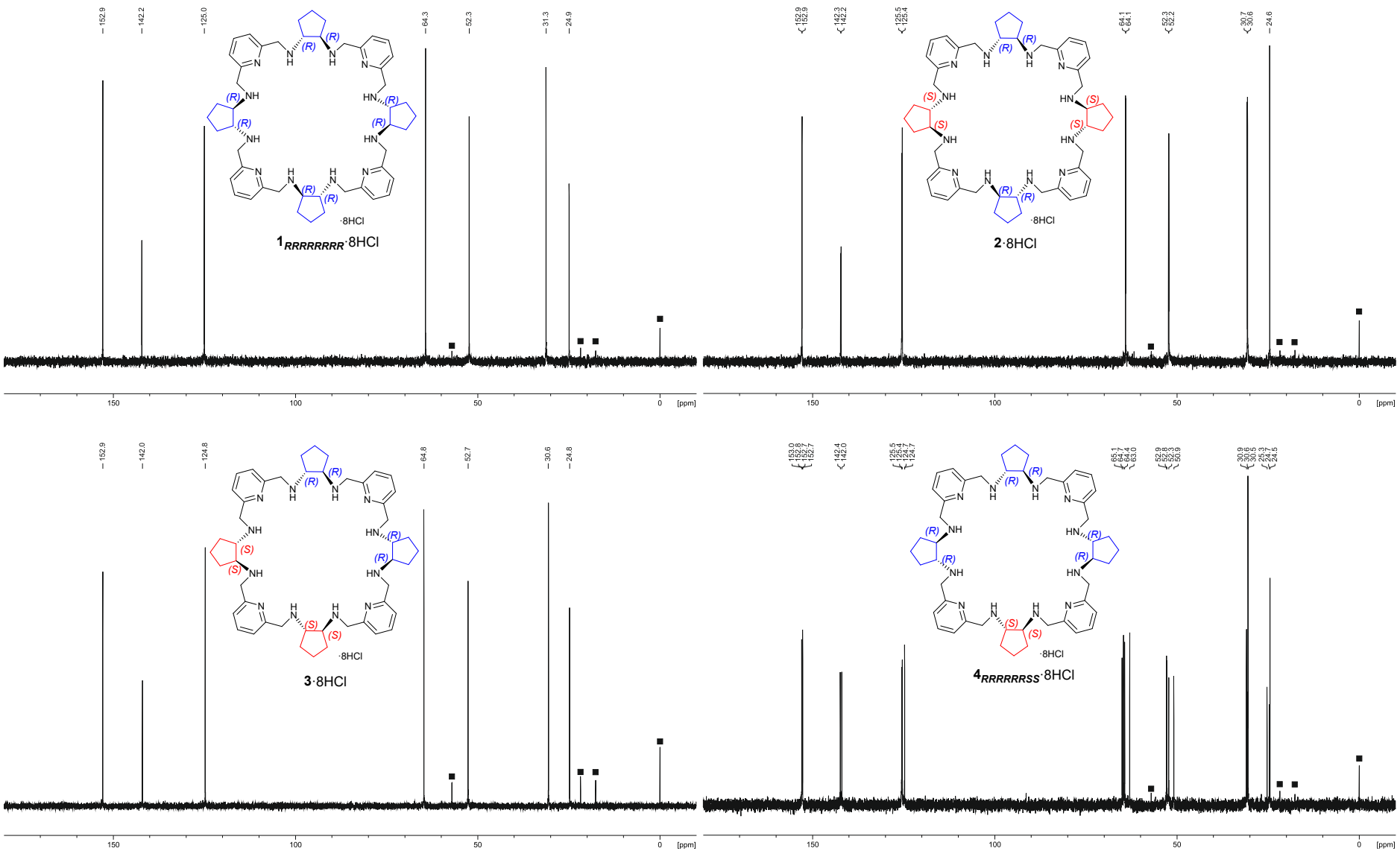

Supporting figure S22. Comparison of $^{13}C\ \{^{1}H\}$ NMR spectra (D_2O, 126 MHz) of protonated salts of diastereomeric macrocyclic amines [(**1**$_{RRRRRRRR}$)H_8]Cl_8, [(**2**)H_8]Cl_8, [(**3**)H_8]Cl_8 and [(**4**$_{RRRRRRSS}$)H_8]Cl_8. Black squares denote DSS signals.

9. Symmetry of macrocycles

Both homochiral enantiomers, $\mathbf{1}_{RRRRRRRR}$ and $\mathbf{1}_{SSSSSSSS}$, possess all their cyclopentane moieties of the same chirality (*RRRRRRRR* or *SSSSSSSS*) and exhibit D_4 effective symmetry in a solution (**figure 1**) which results in their very simple NMR spectra.[12h] These spectra are identical for these two enantiomers and the ^{1}H NMR spectrum gives rise to seven non-exchangeable signals and one resonance of eight equivalent NH groups. The ^{13}C NMR pattern comprises seven well-resolved peaks. The very similar ^{1}H and ^{13}C NMR spectral patterns are also observed in the case of achiral *meso I* 4+4 amine macrocycle **2**.[8a] This heterochiral derivative which is an example of heterochiral diastereomer having four DACP units of alternating opposite *RRSSRRSS* chiralities of their asymmetric carbon atoms. The molecule possesses only S_4 symmetry axis which is a source of a very high effective D_{2d} symmetry of macrocyclic amine **2** in a solution (**figure 1**). The same very high symmetries are also maintained in the case of more rigid protonated derivatives of macrocycles **1** and **2**, $[(\mathbf{1}_{RRRRRRRR})H_8]Cl_8$ / $[(\mathbf{1}_{SSSSSSSS})H_8]Cl_8$ (D_4 symmetry)[12h], and $[(\mathbf{2})H_8]Cl_8$ (D_{2d} symmetry)[8a] (**figure 3, supporting figure S22)** but also $[(\mathbf{1}_{SSSSSSSS})H_8](HSO_4)_4(SO_4)_2$, (**supporting figure S19**) which give rise also to 7 ^{1}H and 7 ^{13}C NMR signals (in D_2O).

In the case of a new macrocycle **3**, which is achiral and represents the second *meso II* form, the homochiral 2+2 *RRRR* and *SSSS* linear halves of macrocyclic molecules are arranged in neighboring fashion and are connected together forming a macrocyclic molecule of *RRRRSSSS* chiralities of their DACP units (**figure 1**). The effective symmetry of macrocycle **3** in a solution is C_{2h} which should theoretically result in doubling of almost all ^{1}H and ^{13} C NMR signals seen in the spectra of highly symmetrical macrocycles **1** and **2** (the only exception is a signal of position **g** which is not doubled- see **figure 1** for labelling).

And indeed, in the ^{1}H NMR spectrum (in D_2O) of protonated derivative $[(\mathbf{3})H_8]Cl_8$ (**figure 3**, **supporting figure 20a**) there are 2 triplets of γ-pyridine protons **a1/a2**, 2 doublets of β-pyridine protons **b1/b2**, 2 AB quartets of methylene protons **d1/d2** as well as each multiplet originating from -CH- or -CH_2- protons of CP rings has its own counterpart i.e. **e1/e2**, $\mathbf{f1_a/f2_a}$ and $\mathbf{f1_e/f2_e}$. As predicted, there is only one multiplet originating from 8 equivalent protons **g**. The ^{13}C NMR spectrum of protonated derivative $[(\mathbf{3})H_8]Cl_8$ show in turn all of its carbon resonances (apart from carbon atom **g**) as twin signals (**supporting figure 20b**). Due to fluxional nature of the free amine macrocycle **3**, which is more flexible in a solution than its protonated derivative $[(\mathbf{3})H_8]Cl_8$, the doubling of signals is less pronounced in its ^{1}H NMR spectrum (**supporting figure 17a**). The respective ^{1}H NMR signals lie closer (**a1/a2**, **b1/b2** and **d1/d2**) and some of them (**e1/e2**, $\mathbf{f1_a/f2_a}$ and $\mathbf{f1_e/f2_e}$) overlap, however even these overlapped multiplets preserve characteristic twin shapes. The ^{13}C NMR spectrum of the free amine macrocycle **3** (**supporting figure 17b**) still displays almost all resonances grouped in pairs, here however, the differences in chemical shifts are smaller than in the case of its protonated derivative **3**·8HCl.

The macrocyclic amine **4** ($\mathbf{4}_{RRRRRRSS}$ and $\mathbf{4}_{SSSSSSRR}$) belongs also to heterochiral compounds. Its molecule comprises three DACP units of the same *RR* or *SS* chirality, whereas the last fourth DACP unit has opposite *SS* or *RR* chirality. The effective symmetry of macrocyclic amine **4**, i.e., $\mathbf{4}_{RRRRRRSS}$ and $\mathbf{4}_{SSSSSSRR}$, is C_2 (**figure 1**). This means that 29 non-exchangeable should theoretically be observed in ^{1}H NMR spectrum and 25 resonances in ^{13}C NMR spectrum. The close inspection of the NMR spectra of both enantiomers of octahydrochloride derivatives $[(\mathbf{4}_{RRRRRRSS})H_8]Cl_8$ and $[(\mathbf{4}_{SSSSSSRR})H_8]Cl_8$ (**figure 3**, **supporting figure 21a**) confirms the C_2 symmetry in a D_2O solution. The ^{13}C NMR spectrum shows 24 signals (only two out of four signals **f1-f4** are not resolved) (**supporting figure 21b**), whereas in the ^{1}H NMR spectrum

(**supporting figure 21a**) some of the signals are overlaid due to smaller differences in chemical shifts in comparison to the ^{13}C NMR spectra. Signals of non-equivalent protons **d1-d4** are overlapped and cover additionally partially the signals of protons **e1-e4** whereas the signals of protons **f1-f4** overlap these of protons **g1-g3**. However, in the aromatic region – 2 triplets of γ-pyridine protons **a1/a2** and 4 doublets of β-pyridine protons **b1-b4** remain well separated. The structures of the neutral forms of free amines $\mathbf{4}_{RRRRRRSS}$ and $\mathbf{4}_{SSSSSSRR}$ have to be more flexible, looser, and less organized than their respective hydrochloride derivatives $[(\mathbf{4}_{RRRRRRSS})H_8]Cl_8$ and $[(\mathbf{4}_{SSSSSSRR})H_8]Cl_8$. They possibly can exist at RT in solutions in many conformations. The dynamic rearrangement of various conformations of the macrocycle averages the contributions to the chemical shifts (such as aromatic ring current effects of pyridine fragments) of various conformers in such a way that the chemical shifts for the different types of pyridine rings and various types of cyclopentane rings are becoming practically equal. This is reflected in their NMR spectra (**supporting figures 18a, b**) where the number of observed signals is much smaller (11 ^{1}H NMR and 14 ^{13}C NMR signals) in comparison to the spectra of their protonated derivatives.

10. Chiral recognition

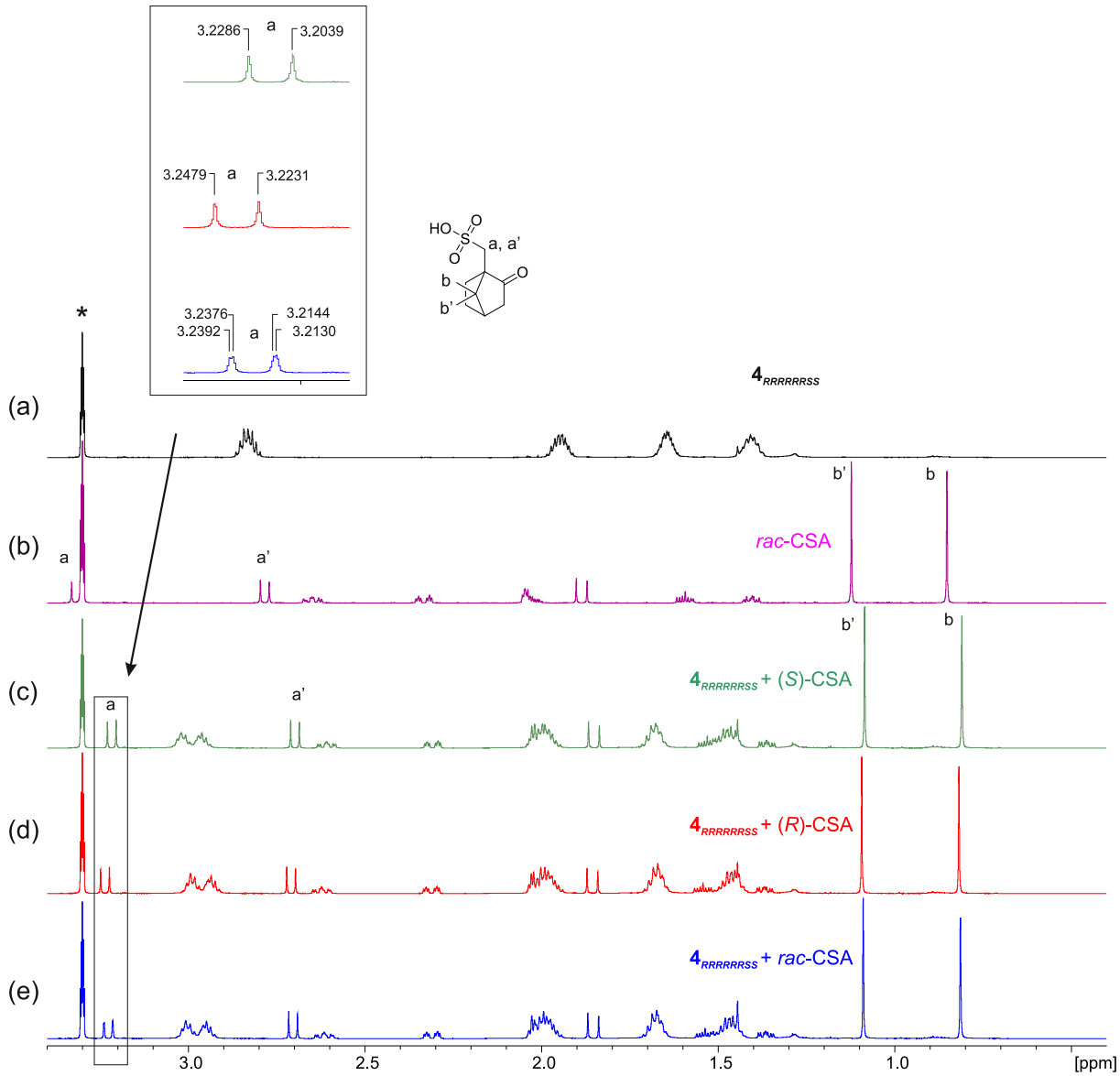

Supporting figure 23a. Fragments of ^{1}H NMR spectra in CD_3OD (500 MHz) of amine $\mathbf{4}_{RRRRRRSS}$ (a), *rac*-CAS (b), a mixture of amine $\mathbf{4}_{RRRRRRSS}$ and (*S*)-CAS (c), a mixture of amine $\mathbf{4}_{RRRRRRSS}$ and (*R*)-CAS (d) and mixture of amine $\mathbf{4}_{RRRRRRSS}$ and *rac*-CAS (e). The doubling of respective signal of proton **a** of *rac*-CSA is shown above in the frame.

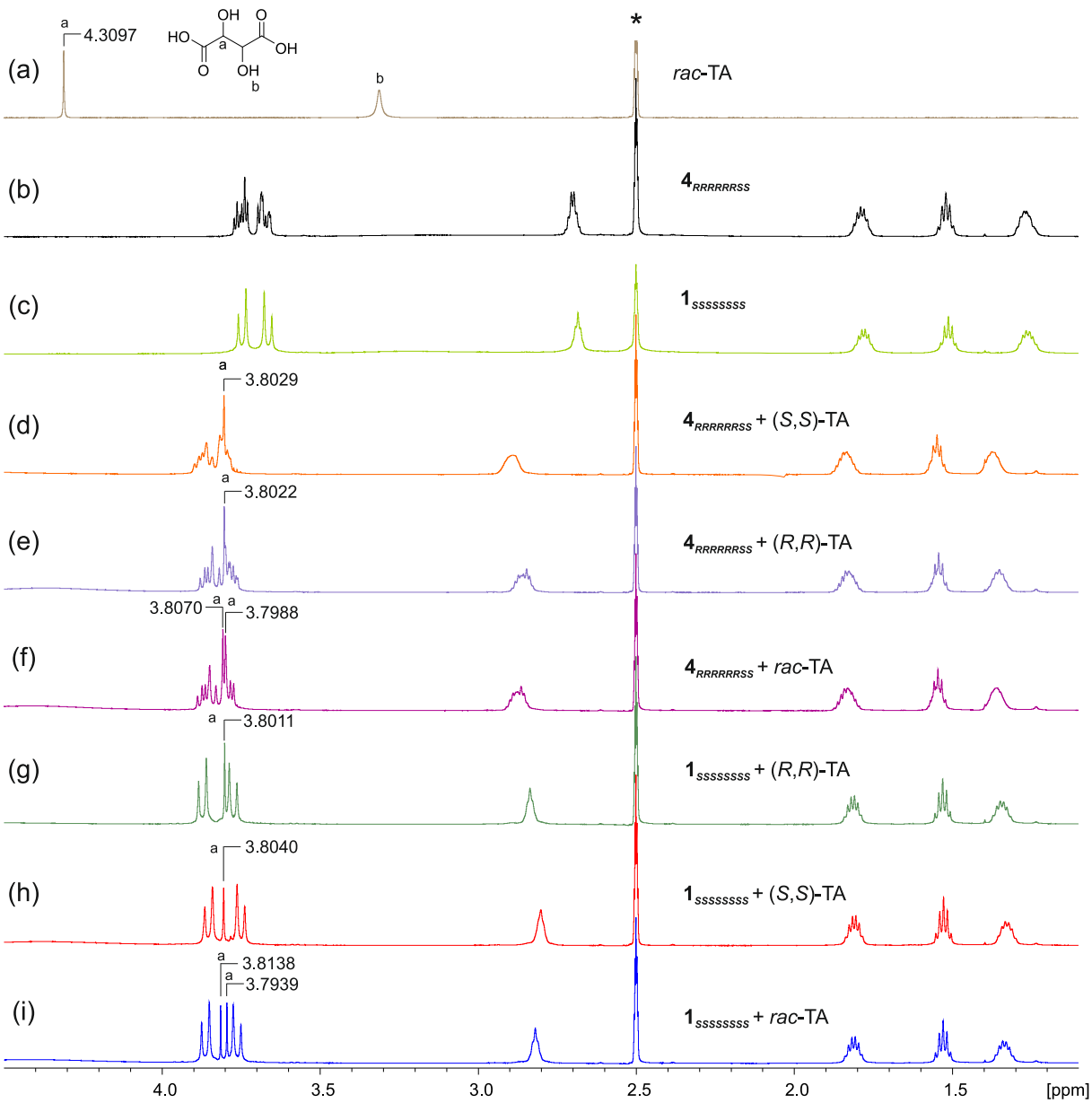

Supporting figure 23b. Fragments of ^{1}H NMR spectra in DMSO-$_{d6}$ (500 MHz) of *rac*-TA (a), amine **4**$_{RRRRRRSS}$ (b), amine **1**$_{SSSSSSSS}$ (c), a mixture of amine **4**$_{RRRRRRSS}$ and (*S,S*)-TA (d), a mixture of amine **4**$_{RRRRRRSS}$ and (*R,R*)-TA (e), a mixture of amine **4**$_{RRRRRRSS}$ and *rac*-TA (f), a mixture of amine **1**$_{SSSSSSSS}$ and (*R,R*)-TA (g), a mixture of amine **1**$_{SSSSSSSS}$ and (*S,S*)-TA (h) and a mixture of amine **1**$_{SSSSSSSS}$ and *rac*-TA (i) .The doubling of respective signal of proton **a** of *rac*-TA show spectra (f) and (i).